

Plasmonique moléculaire : du facteur de Purcell à la plasmonique quantique

G. Colas des Francs

Laboratoire Interdisciplinaire Carnot de Bourgogne (ICB)

CNRS/Université Bourgogne-Franche Comté

Dijon - France



*Ecole thématique plasmonique moléculaire et
spectroscopies exaltées - Toulouse, 2016*



Light/matter interaction at the nanoscale

I] Introduction : motivations and difficulties

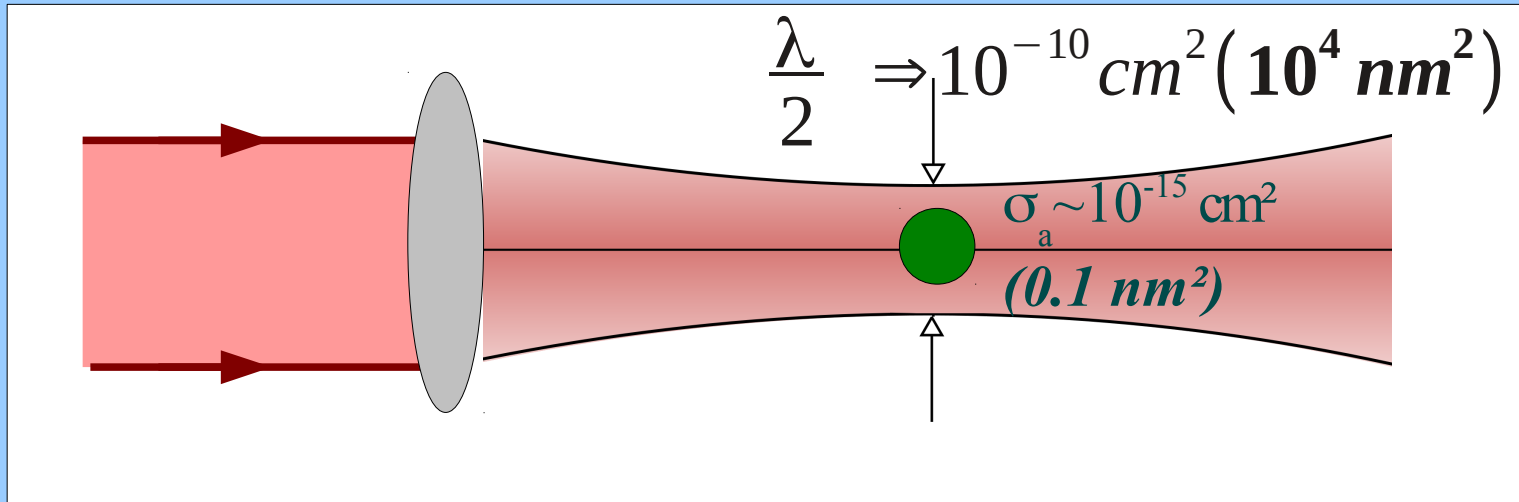
II] Plasmonic Purcell factor (classical approach)

- 1) Delocalized plasmons (SPP)
- 2) Localized plasmon (LSP)

III] Quantum plasmonics

- 1) Effective Hamiltonian
- 2) Strong coupling (emitter-LSP)

Light/matter interaction at the nanoscale



Gaussian beam

$$A_{eff} = \pi w_0^2$$

Absorption cross-section

$$\sigma_a$$

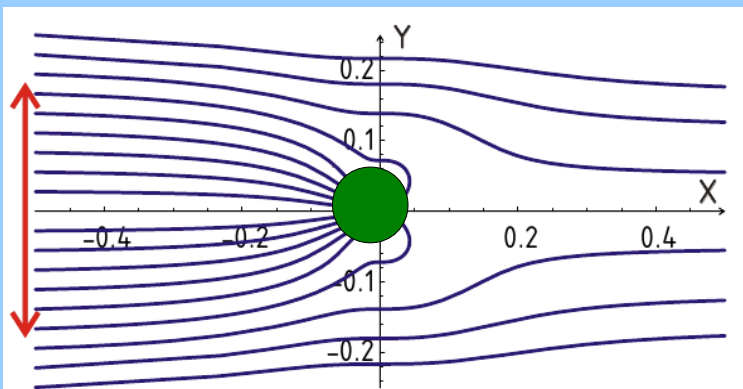
cooperativity $C_0 = \frac{\sigma_a}{A_{eff}} \sim 10^{-3}$

Strategies

Low T°C (<10K)

$$\sigma_a \sim 3\lambda^2/2\pi \sim 10^{-10} \text{ cm}^2$$

($\phi \sim 100x$ molecule size!)

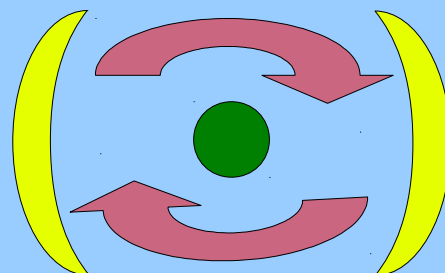


(a) Dipole out off plane (in z)

Paul, Fischer

Light absorption by a dipole, Society Physics
Uspekhi **26**, 923 (1983)

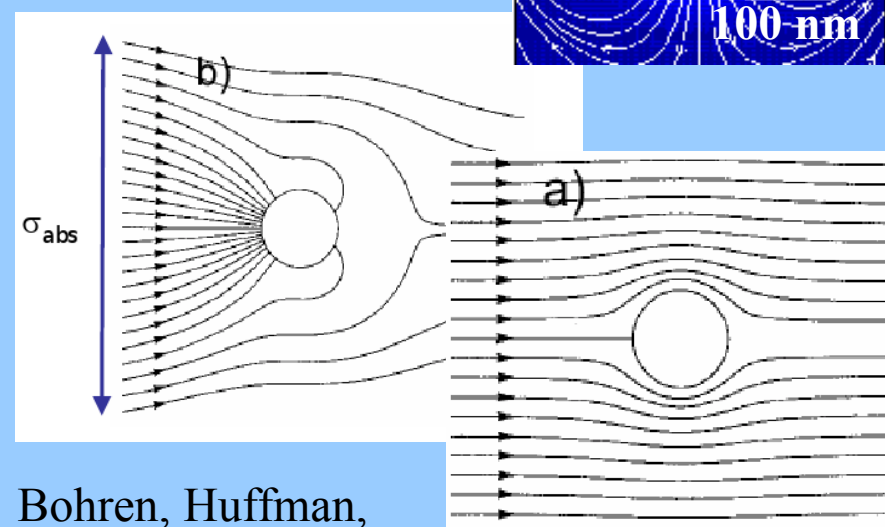
Cavity quantum
electrodynamics
(cQED)



$$C = 4C_0 \frac{\mathcal{F}}{\pi}$$

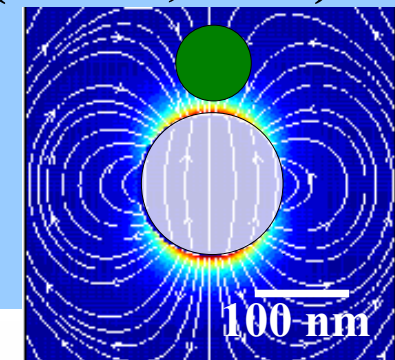
Intensity
enh.

Round
trip



Bohren, Huffman,
Absorption and Scattering of Light by Small
Particles, Wiley, New York 1983

Surface enhanced
spectroscopies
(SERS, SEF)



Purcell factor

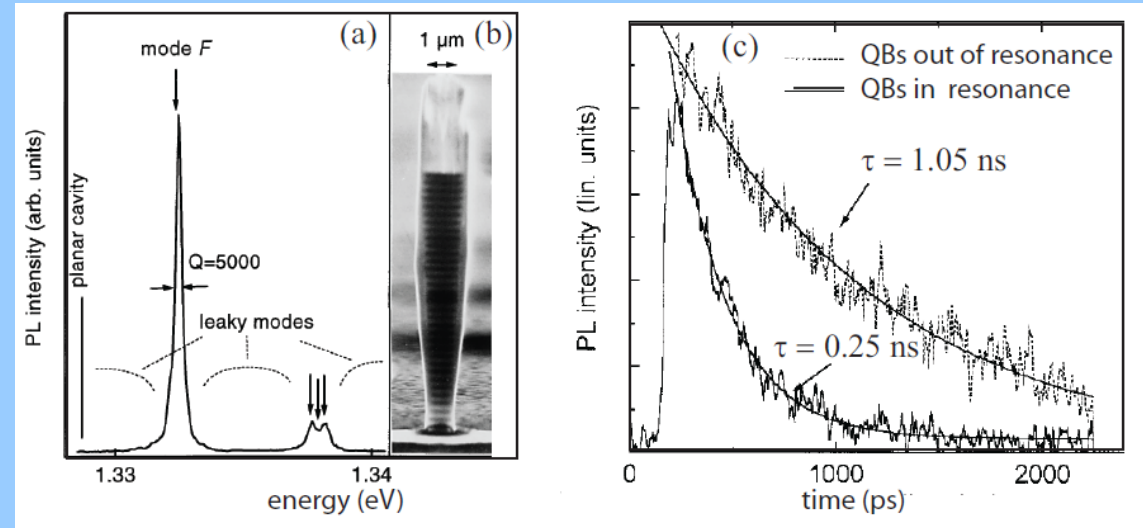
Proceedings of the American Physical Society

MINUTES OF THE SPRING MEETING AT CAMBRIDGE, APRIL 25-27, 1946

B10. Spontaneous Emission Probabilities at Radio Frequencies. E. M. PURCELL, *Harvard University*.—For nuclear magnetic moment transitions at radio frequencies the probability of spontaneous emission, computed from

$$A_\nu = (8\pi\nu^2/c^3)h\nu(8\pi^3\mu^2/3h^2) \text{ sec.}^{-1},$$

is so small that this process is not effective in bringing a spin system into thermal equilibrium with its surroundings. At 300°K, for $\nu = 10^7 \text{ sec.}^{-1}$, $\mu = 1$ nuclear magneton, the corresponding relaxation time would be 5×10^{21} seconds! However, for a system coupled to a resonant electrical circuit, the factor $8\pi\nu^2/c^3$ no longer gives correctly the number of radiation oscillators per unit volume, in unit frequency range, there being now *one* oscillator in the frequency range ν/Q associated with the circuit. The spontaneous emission probability is thereby increased, and the relaxation time reduced, by a factor $f = 3Q\lambda^3/4\pi^2V$, where V is the volume of the resonator. If a is a dimension characteristic of the circuit so that $V \sim a^3$, and if δ is the skin-depth at frequency ν , $f \sim \lambda^3/a^2\delta$. For a non-resonant circuit $f \sim \lambda^3/a^3$, and for $a < \delta$ it can be shown that $f \sim \lambda^3/a\delta^2$. If small metallic particles, of diameter 10^{-3} cm are mixed with a nuclear-magnetic medium at room temperature, spontaneous emission should establish thermal equilibrium in a time of the order of minutes, for $\nu = 10^7 \text{ sec.}^{-1}$.

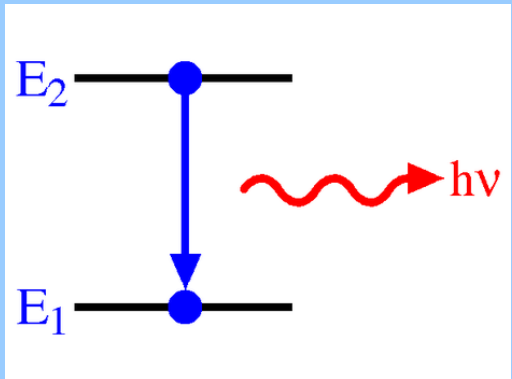


Gérard, Gayral, J. Light. Tech. (1999) □

Purcell, 1946

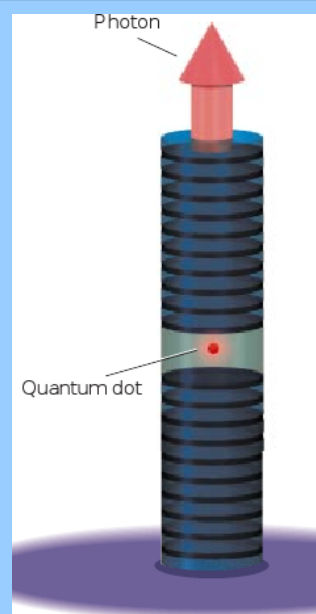
Control of the spontaneous emission – Purcell factor

Fermi's golden rule

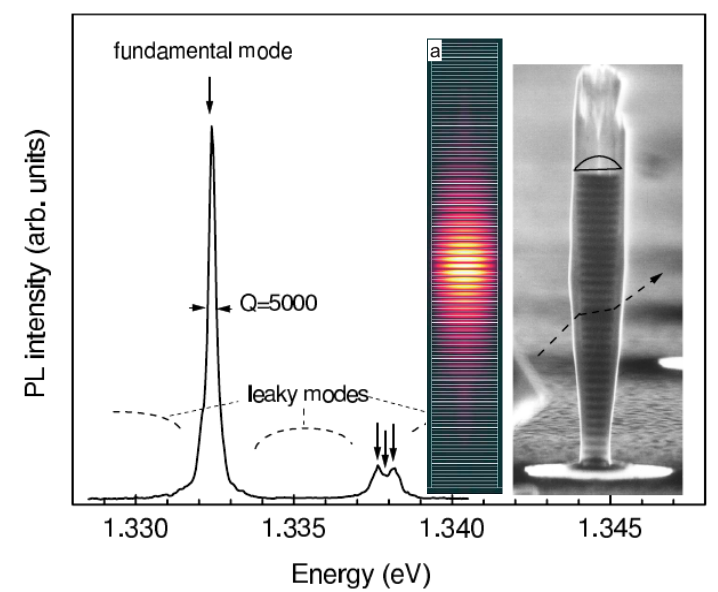


$$\Gamma = \frac{\pi \omega}{\hbar \epsilon_0} |\mathbf{p}|^2 \rho(\mathbf{r}_m, \omega)$$

Density of modes



Purcell factor

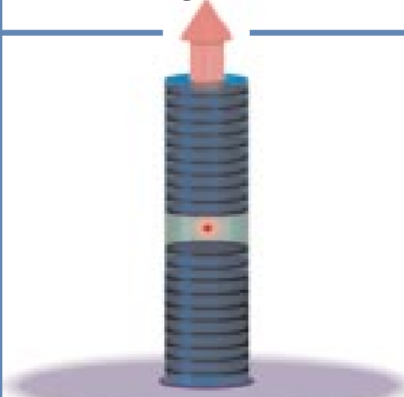
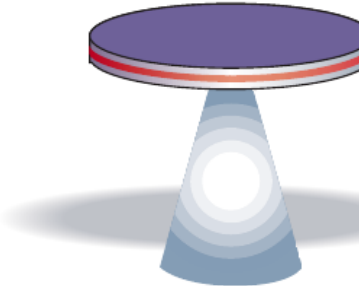
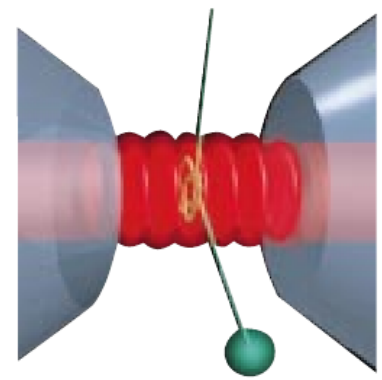
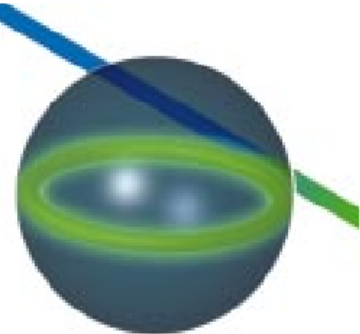
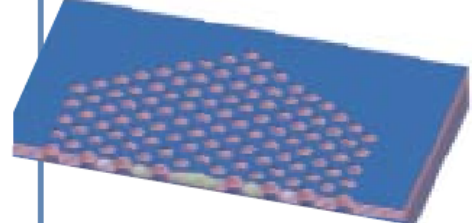


Given cavity

mode

$$F_p = \frac{\Gamma}{\Gamma_0} = \frac{3}{4\pi^2} \left(\frac{\lambda}{n} \right)^3 \frac{Q_{cav}}{V_{mode}}$$

Micro-optical cavities

	Fabry-Perot	Whispering gallery	Photonic crystal
High Q	 Q: 2,000 V: $5 (\lambda/n)^3$	 Q: 12,000 V: $6 (\lambda/n)^3$	 Q _{III-V} : 7,000 Q _{Poly} : 1.3×10^5
Ultrahigh Q	 F: 4.8×10^5 V: $1,690 \mu\text{m}^3$	 Q: 8×10^9 V: $3,000 \mu\text{m}^3$	Vahala Nature 424, 839(2003)  Q: 10^8

Low threshold/thresholdless laser

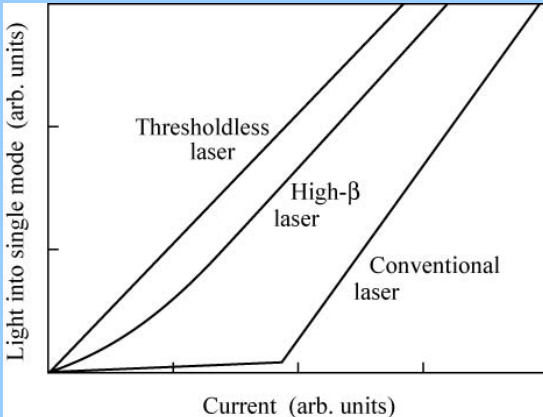
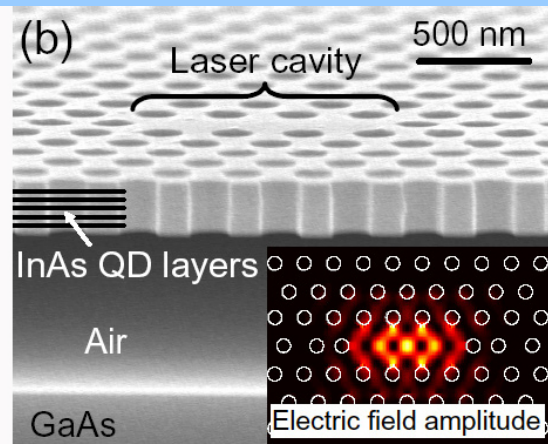
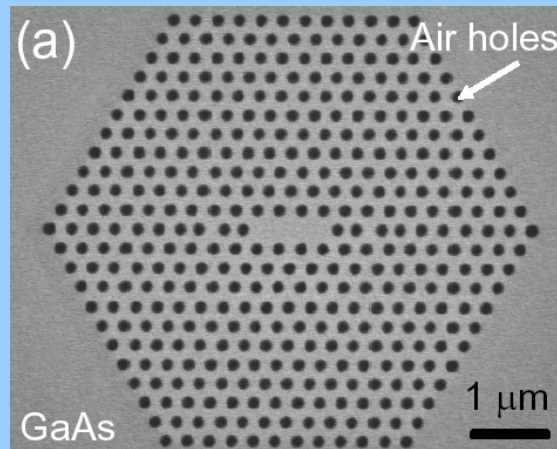
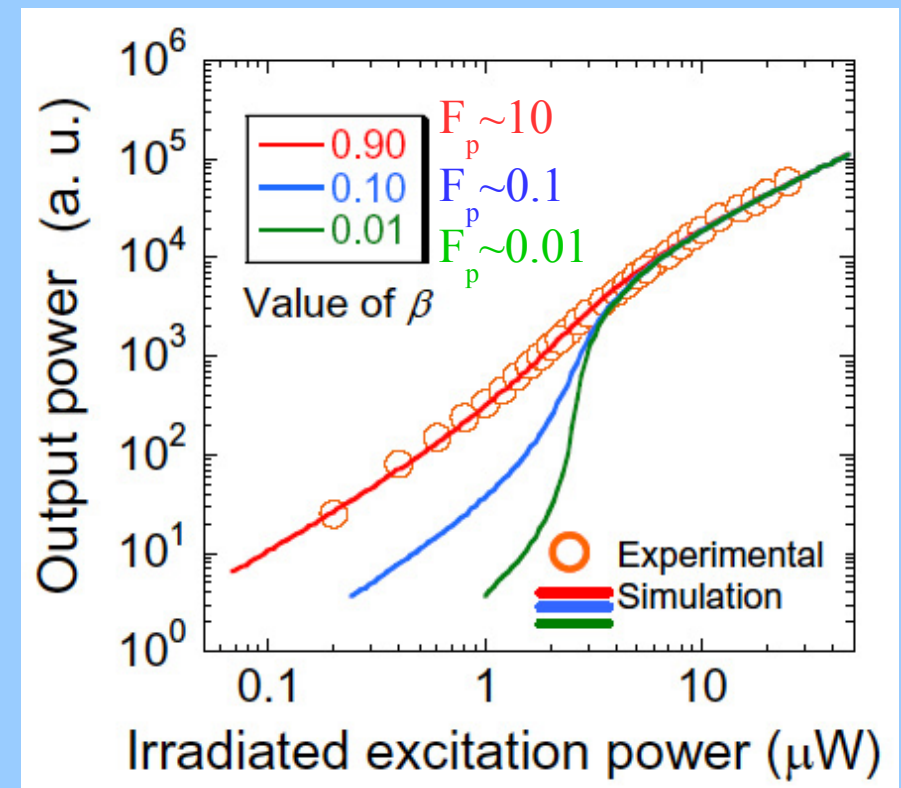


Fig. 15.14. Light-power-versus-current curves for single spatial-mode emission from a (i) conventional laser, (ii) a high β -factor laser, and (iii) a thresholdless laser. The conventional laser has a distinct current threshold. The high β -factor laser has a less distinct threshold. It would be noticeable in the spectrum and device modulation speed, however. A hypothetical thresholdless laser would have a β close to 1, and would somehow suppress all other lossy emission until the carrier density required for gain (or at least transparency) was achieved.

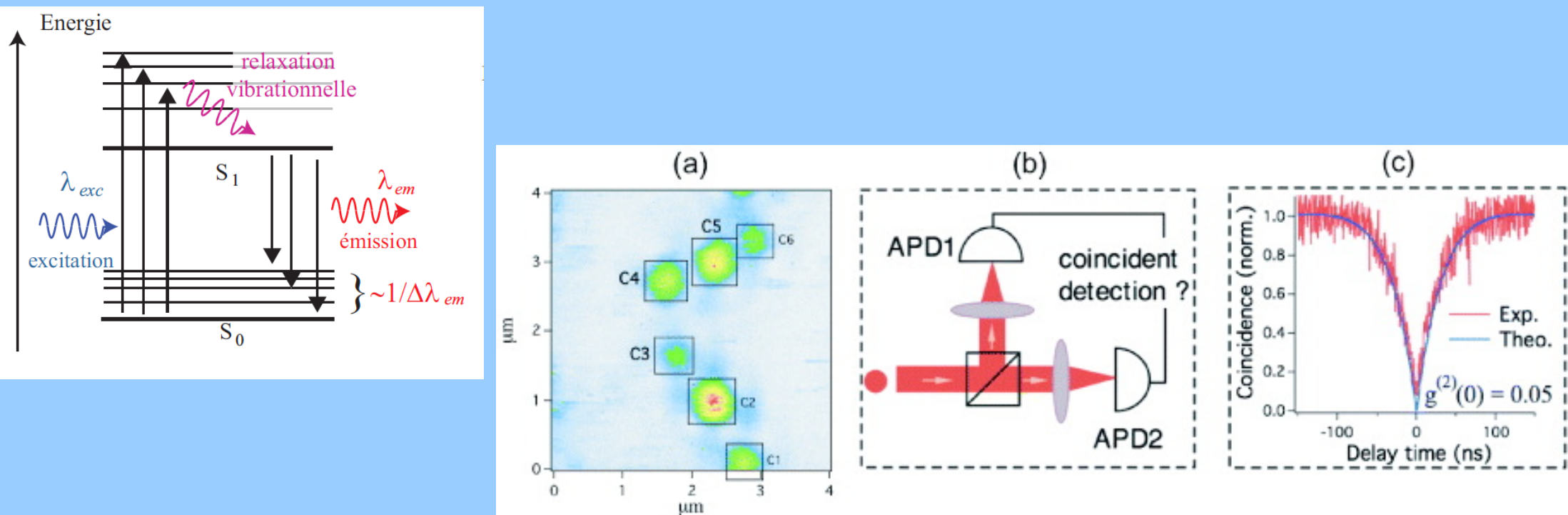
E. F. Schubert
Light-Emitting Diodes (Cambridge Univ. Press)
www.LightEmittingDiodes.org



$$\beta = \frac{\Gamma_{cav}}{\Gamma_{tot}} \approx \frac{F_p}{1 + F_p}$$



Single photon source



Roch, Treussart (ENS Cachan)

Specifications

- Photon energy (wavelength)
- On demand single photon, repetition rate
- Indistinguishable photons

Indistinguishable single photons

$$\Gamma = \frac{1}{T_1}$$

Population decay rate
(inverse of the measure lifetime)

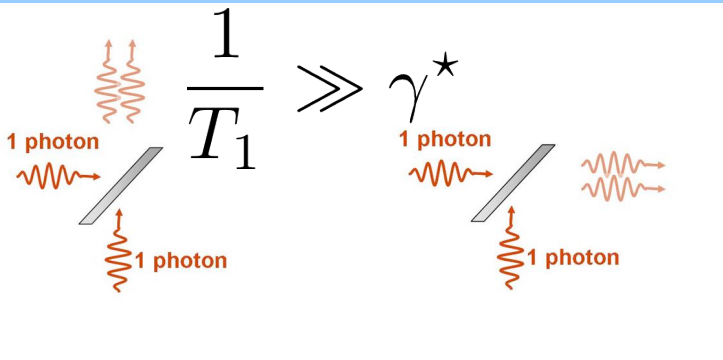
$$\Gamma_{coh} = \frac{1}{T_2}$$

Coherence rate
(dipole lifetime)

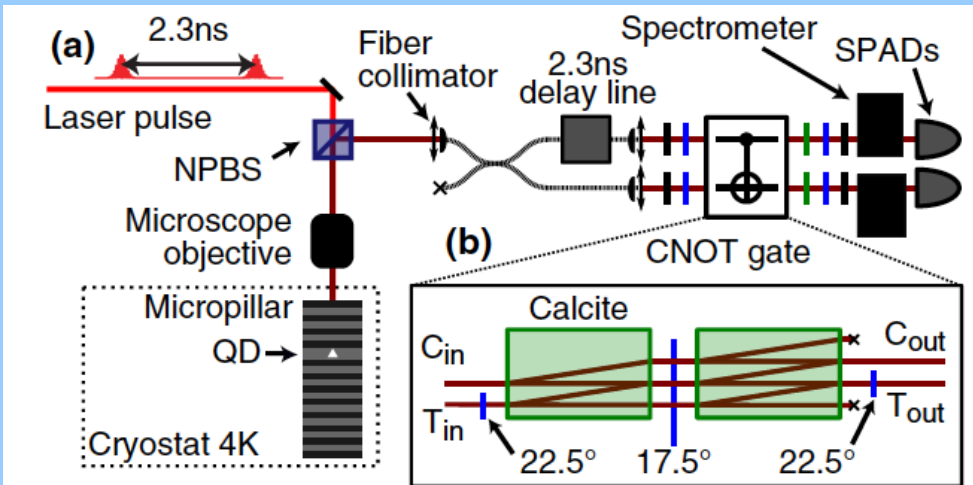
$$\frac{1}{T_2} = \frac{1}{2T_1} + \gamma^*$$

Indistinguishability

$$\frac{T_2}{2T_1}$$

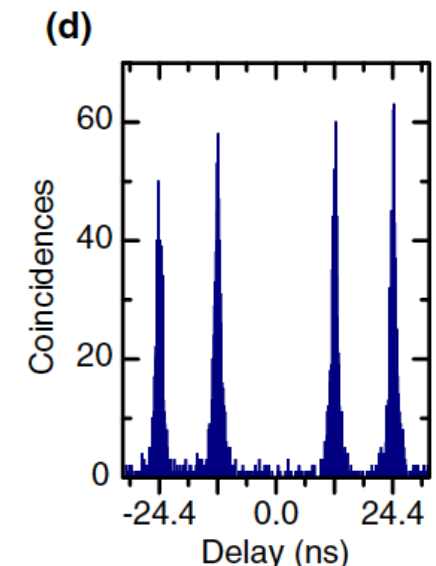


Coalescence effect



C-NOT gate
- purely quantum
- universal gate

Fp~4

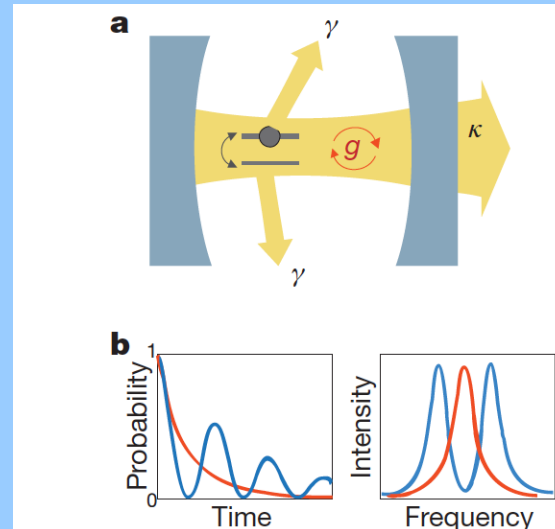


Senellart, PRL 110, 250501 (2013)

Weak and strong coupling regimes

Weak coupling

$$F_p = \frac{\Gamma_{cav}}{n_1 \Gamma_0}$$
$$= \frac{3}{4\pi^2} \left(\frac{\lambda}{n_1} \right)^3 \frac{Q_{cav}}{V_{mode}}$$



Strong coupling

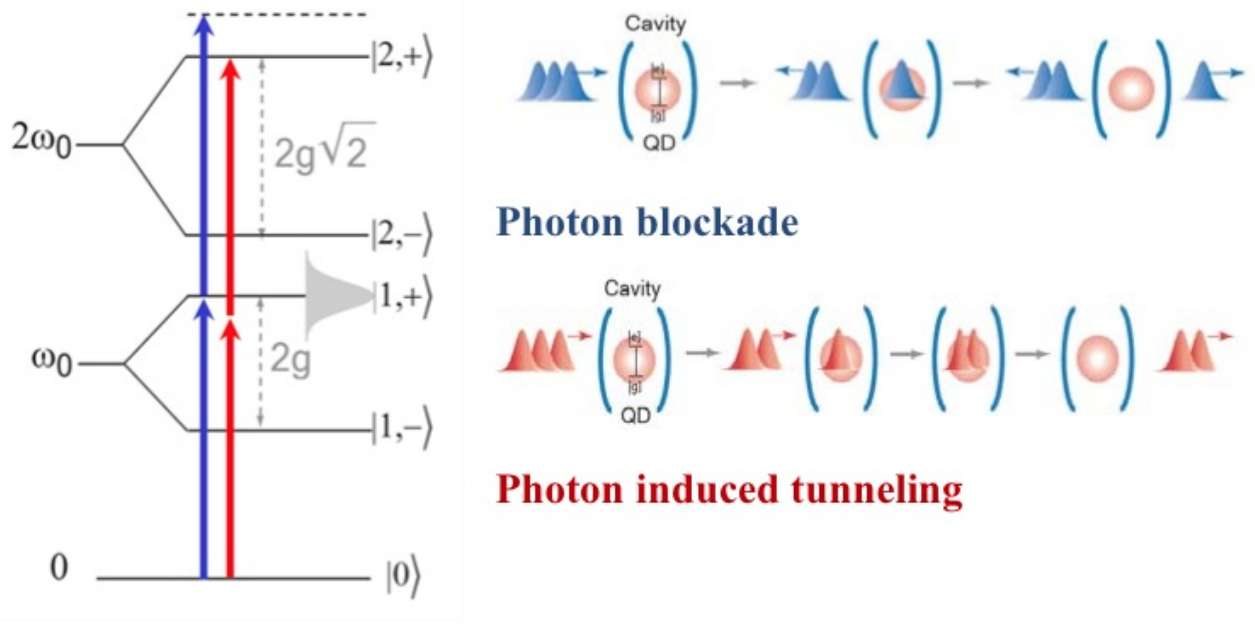
Coupling strength (g)
 \gg
losses (Γ_0, K_{cav})

$$C = \frac{g^2}{2\kappa n_1 \Gamma_0} \gg 1$$

Note : Fabry-Perot cavity

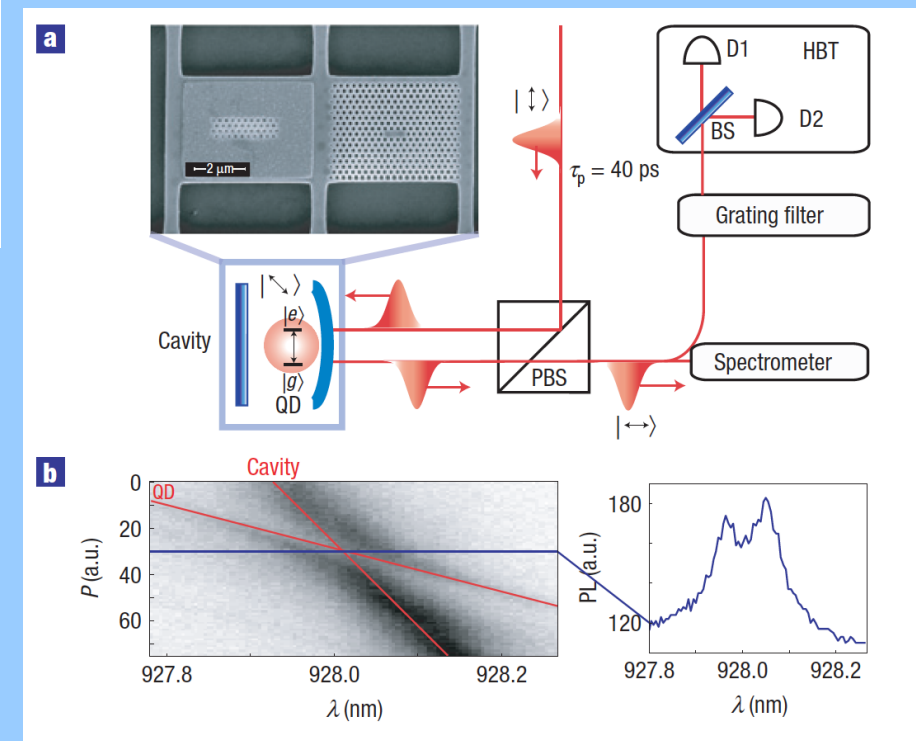
$$C = 4C_0 \frac{\mathcal{F}}{\pi} \quad F_p = 2C$$

Strong coupling regime

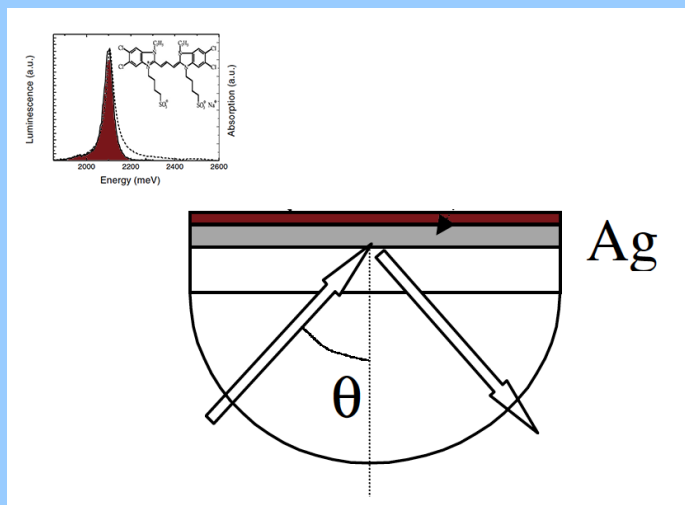


Vuckovic, Nature Physics 4, 859 (2008)

Generation of
non classical photon states

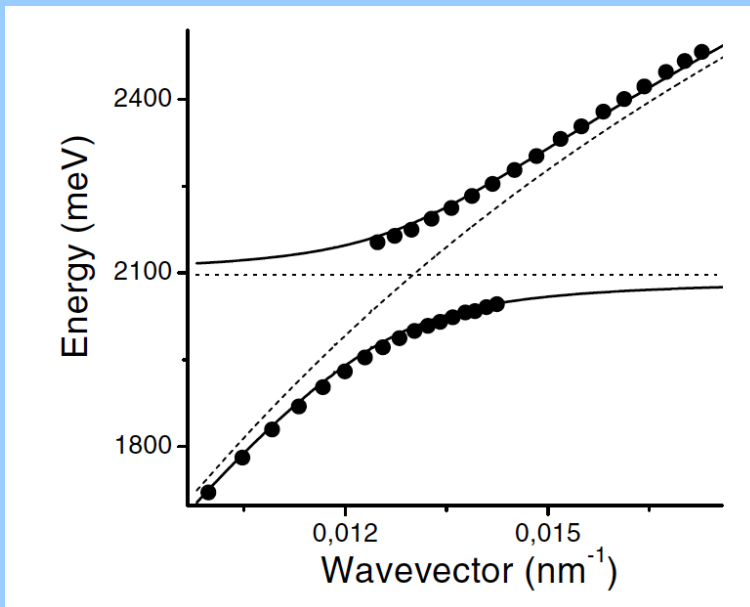


Strong coupling regime in plasmonics

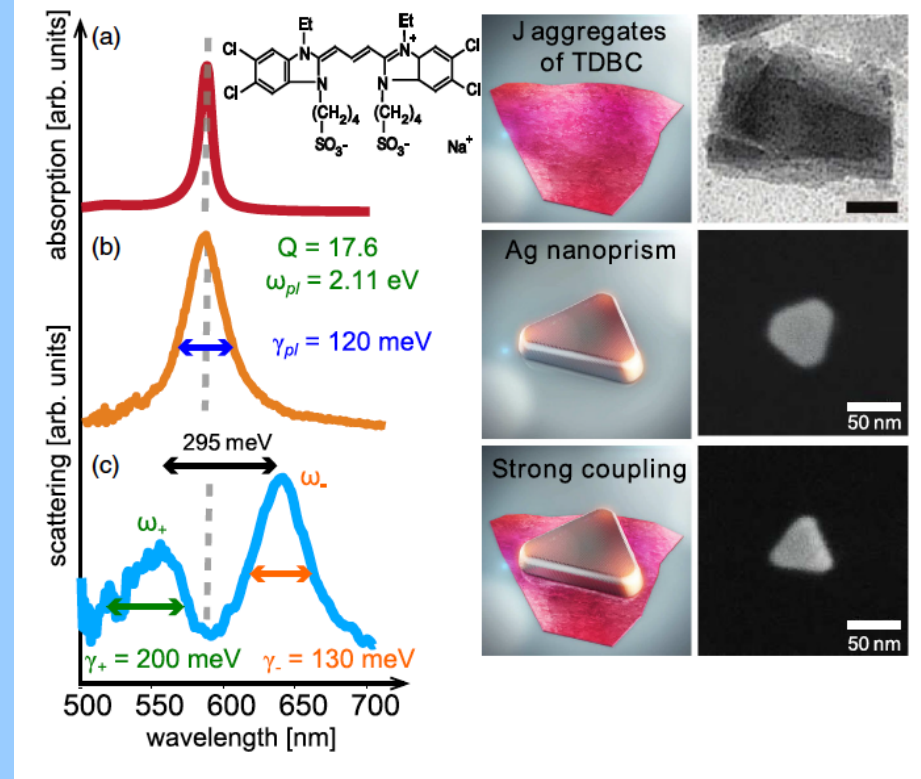


Delocalized SPP

Belessa *et al*,
PRL 93, 0364041
(2004)



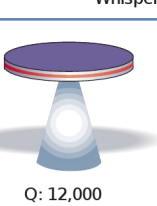
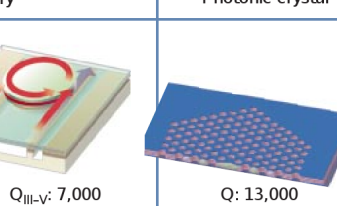
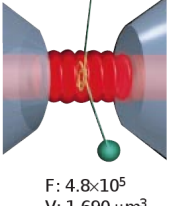
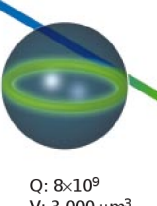
Localized SPP

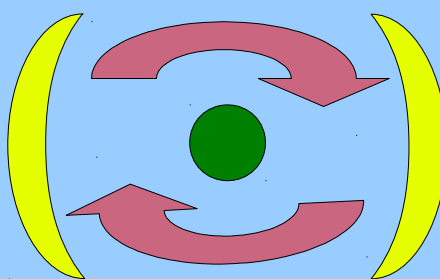


Zengi *et al*, PRL 114, 157401 (2015)

Towards integrated quantum nanophotonics

Cavity quantum electrodynamics (cQED)

	Fabry-Perot	Whispering gallery	Photonic crystal
High Q	 Q: 2,000 V: $5 (\lambda/n)^3$	 Q: 12,000 V: $6 (\lambda/n)^3$	 Q _{III-V} : 7,000 Q _{Poly} : 1.3×10^5
Ultrahigh Q	 F: 4.8×10^5 V: $1,690 \mu\text{m}^3$	 Q: 8×10^9 V: $3,000 \mu\text{m}^3$	 Q: 10^8

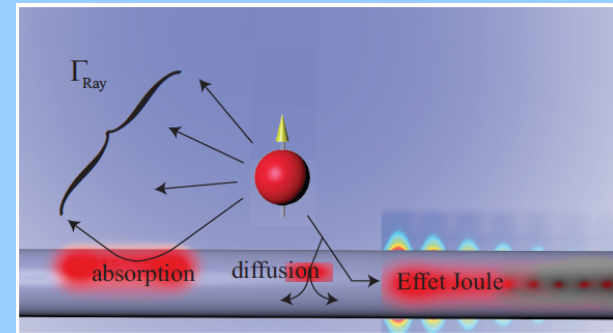


*Duration of interaction
(high Q)*

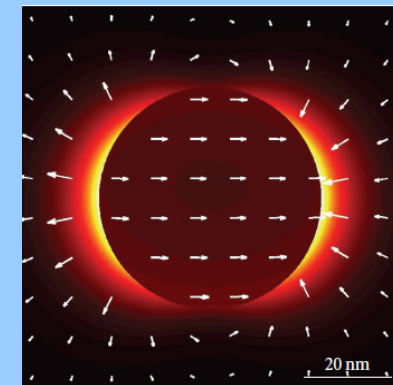
Purcell factor

$$F_p = \frac{\Gamma}{n_1 \Gamma_{tot}} = \frac{3}{4\pi^2} \left(\frac{\lambda}{n_1} \right)^3 \frac{Q}{V_{eff}}$$

Quantum plasmonics (cavityless QED)



*Volume of interaction
(sub-λ)*



Derivation of the Purcell factor

Fermi rule
(weak coupling regime)

$$\Gamma(\mathbf{r}) = \frac{2\pi}{\hbar^2} \sum_{\mathbf{k}_n} |\langle a, \mathbf{k}_n | H_I | b, 0 \rangle|^2 \delta(\omega_{em} - \omega_{\mathbf{kn}})$$

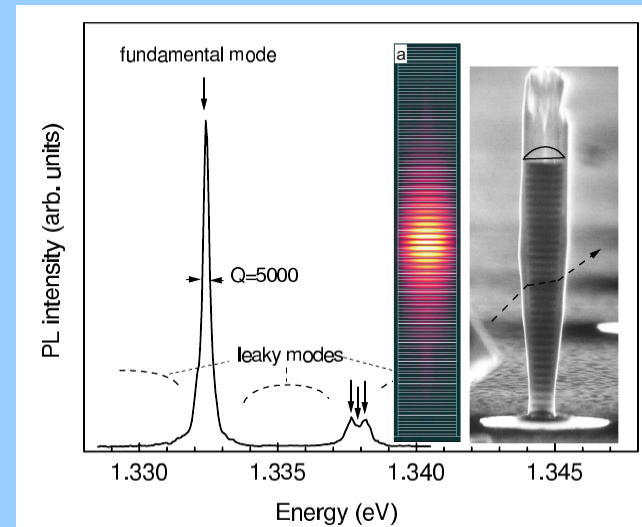
$$H_I = -\hat{\mathbf{p}} \cdot \hat{\mathbf{E}}(\mathbf{r})$$

$$\mathbf{E}_{cav}(\mathbf{r}, t) = i \sqrt{\frac{\hbar \omega_c}{2\varepsilon_0 \varepsilon_1 V}} \mathbf{f}(\mathbf{r}) e^{-i\omega_c t} + c.c$$

$$\delta(\omega - \omega_c) \rightarrow N(\omega) = \frac{1}{\pi} \frac{\kappa_{cav}/2}{(\omega - \omega_c)^2 + \kappa_{cav}^2/4}$$

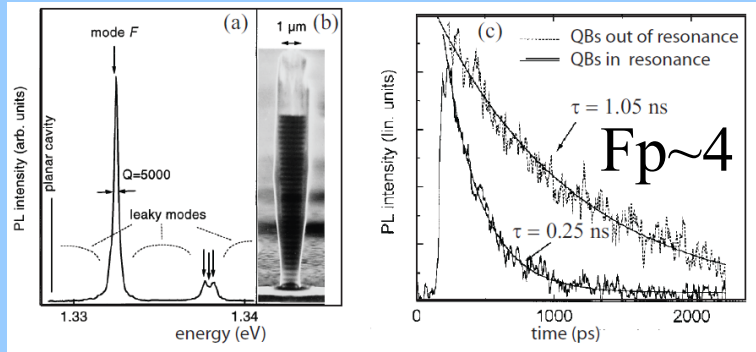
$$N(\omega) = \frac{2Q}{\pi\omega_c} \frac{1}{1 + 4Q^2(\frac{\omega - \omega_c}{\omega_c})^2}$$

$$\frac{\Gamma_{cav}}{n_1 \Gamma_0} = \frac{3}{4\pi^2} \left(\frac{\lambda_{em}}{n_1} \right)^3 \frac{Q}{V} \frac{|\mathbf{u} \cdot \mathbf{f}(\mathbf{r})|^2}{1 + 4Q^2(\frac{\omega_{em} - \omega_c}{\omega_c})^2}$$



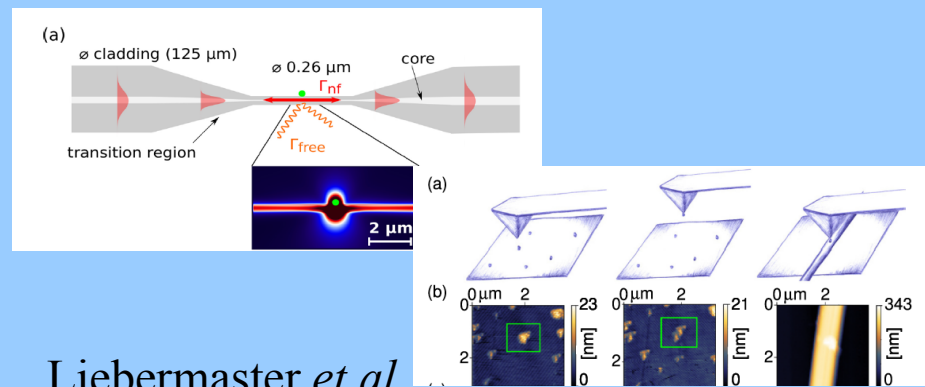
1D, 2D and 3D Purcell factor

Optical μ -cavity (3D confinement)



$$F_p = \frac{\Gamma_{cav}}{n_1 \Gamma_0} = \frac{3}{4\pi^2} \left(\frac{\lambda_{em}}{n_1} \right)^3 \frac{Q}{V_{eff}}$$

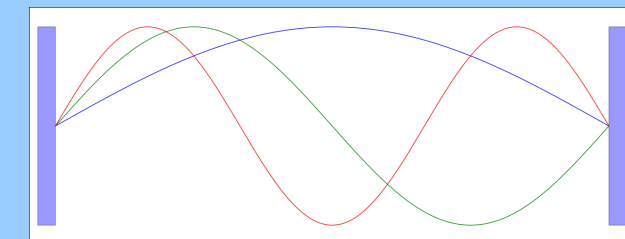
Nanofiber (2D confinement)



Liebermaster *et al*,
Appl. Phys. Lett. **104**, 031101 (2014)

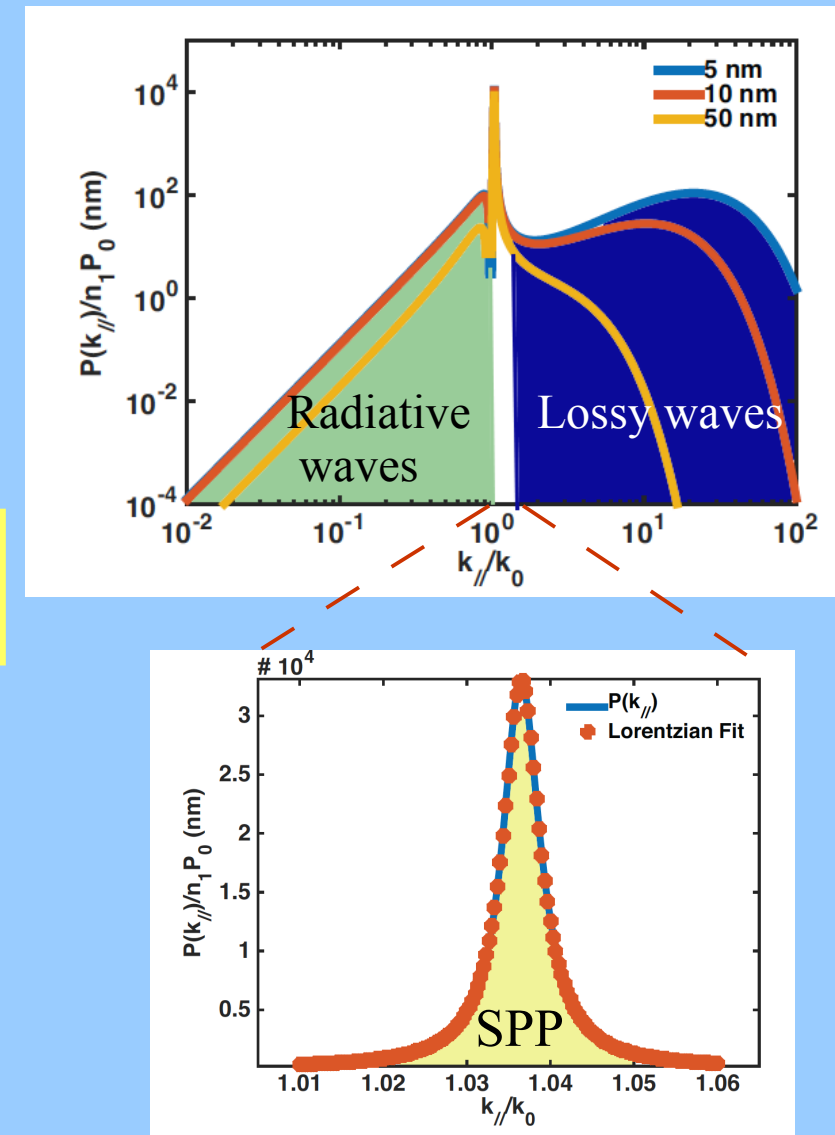
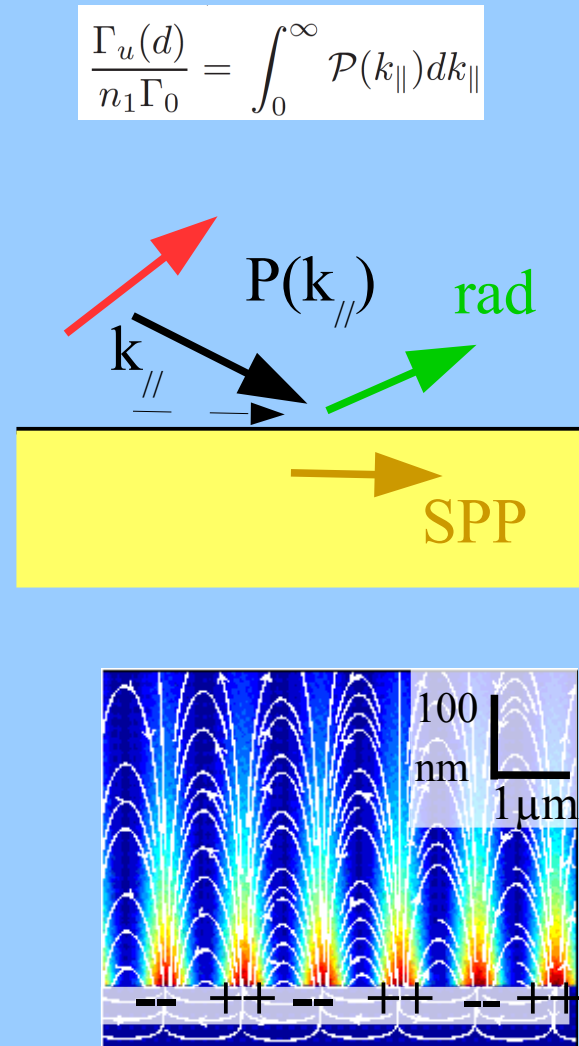
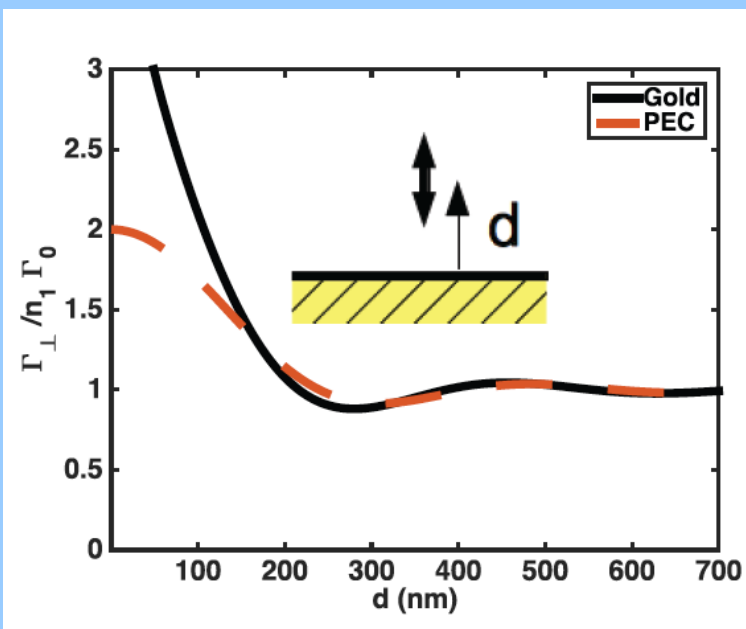
$$F_p = \frac{\Gamma_{guided}}{n_1 \Gamma_0} = \frac{3}{4\pi} \frac{(\lambda_{em}/n_1)^2}{A_{eff}} \frac{n_g}{n_1}$$

Coupling efficiency $\sim 10\%$
(ideally 36%)



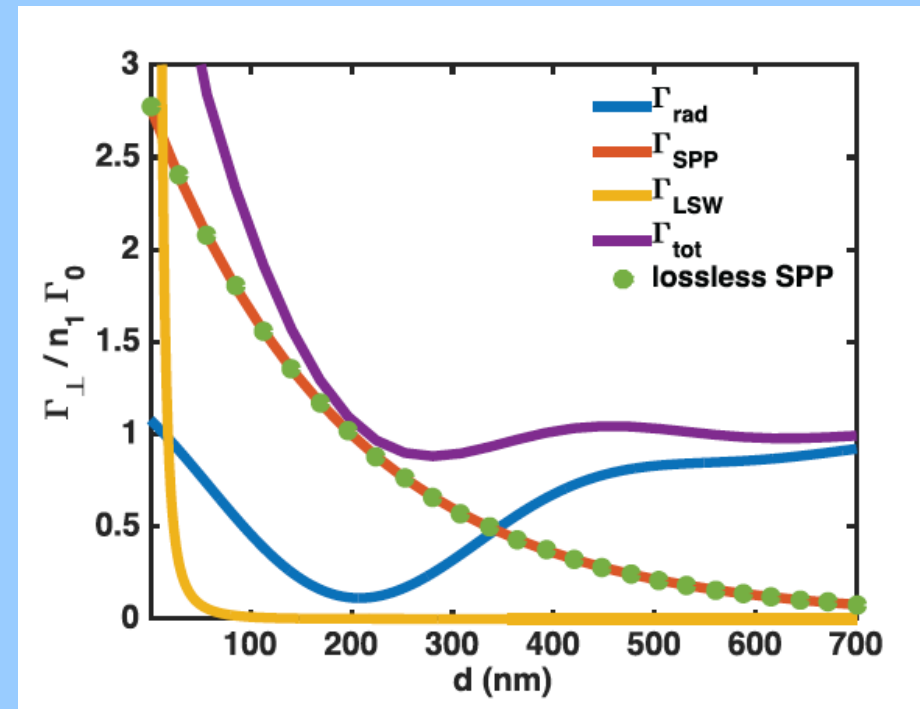
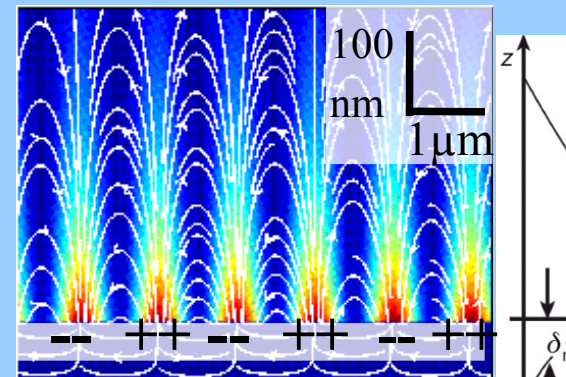
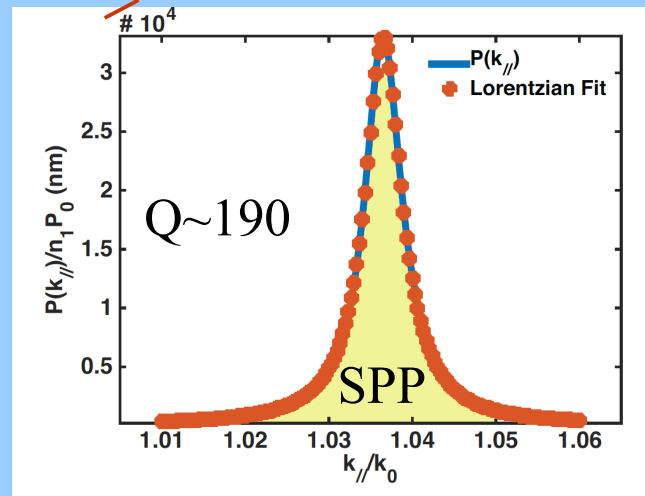
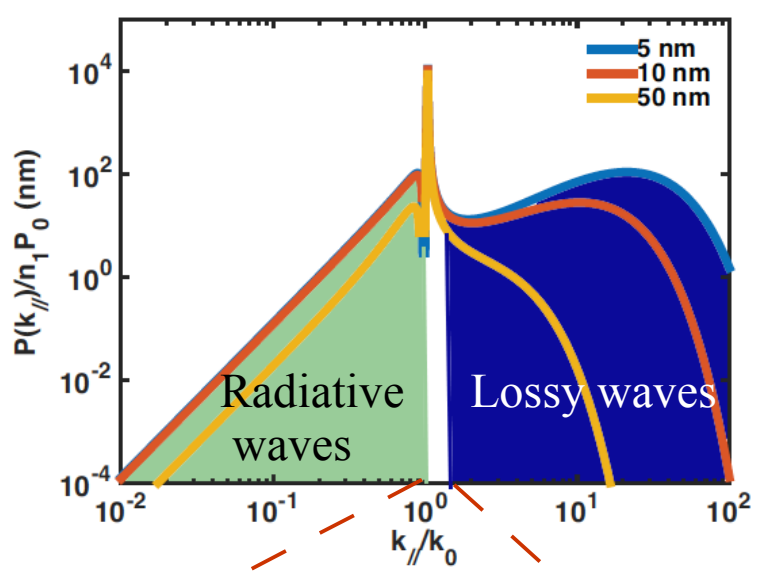
$$F_p = \frac{\Gamma_{guided}}{n_1 \Gamma_0} = \frac{3}{4} \frac{(\lambda_{em}/n_1)}{L_{eff}} \frac{n_{eff} n_g}{n_1^2}$$

The planar film revisited

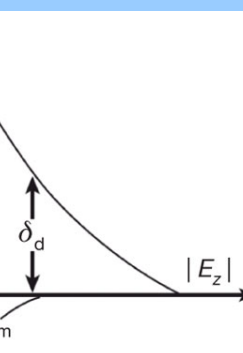


Adapted from
Barnes, J. Modern Optics (1998)

Decay channels

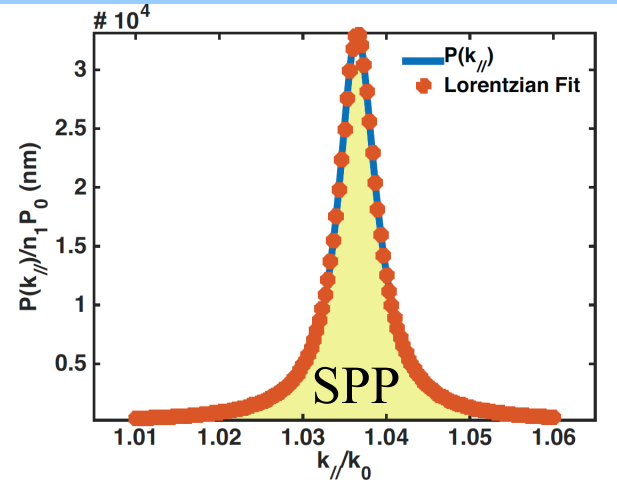


$$L_{eff} = \frac{\int |E(z)|^2 dz}{Max[|E(z)|^2]} = \int_0^\infty e^{-2z/\delta} dz = \frac{\delta}{2}$$



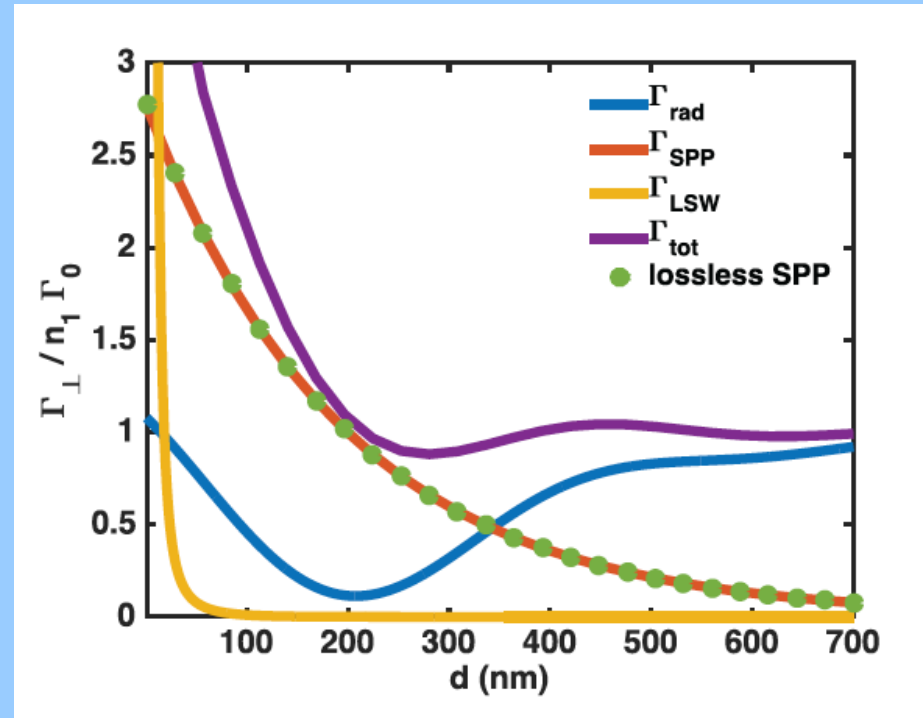
$L_{eff} \sim$ penetration depth in air
 $\sim 0.5 \frac{\lambda_{SPP}}{2}$

Losses



$$\text{Lorentzian} \Rightarrow \frac{\Gamma_{SPP}}{n_1 \Gamma_0} = \frac{\pi}{2} \frac{\mathcal{P}(k_{SPP})}{L_{SPP}}$$

(lossy metal)

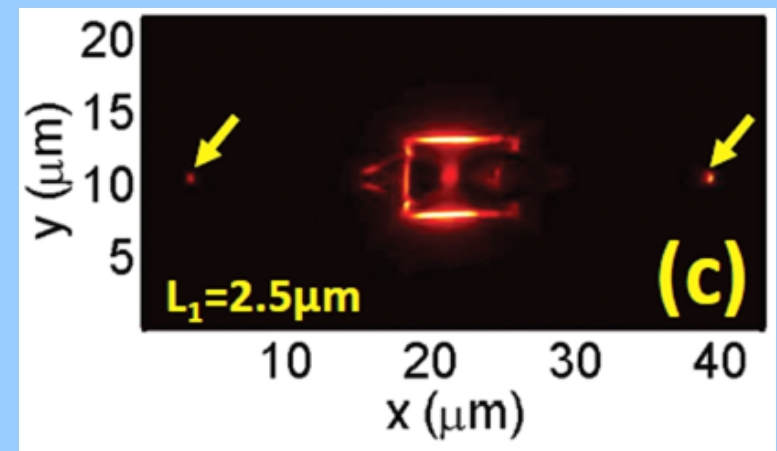
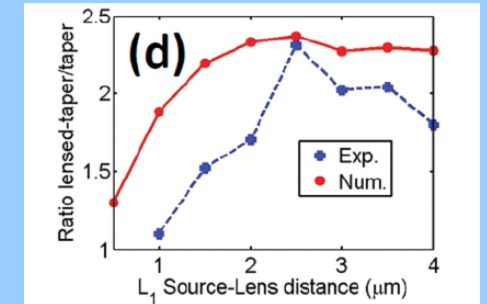
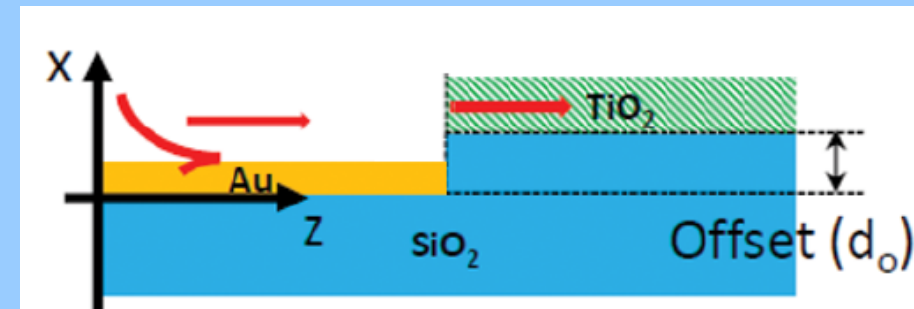
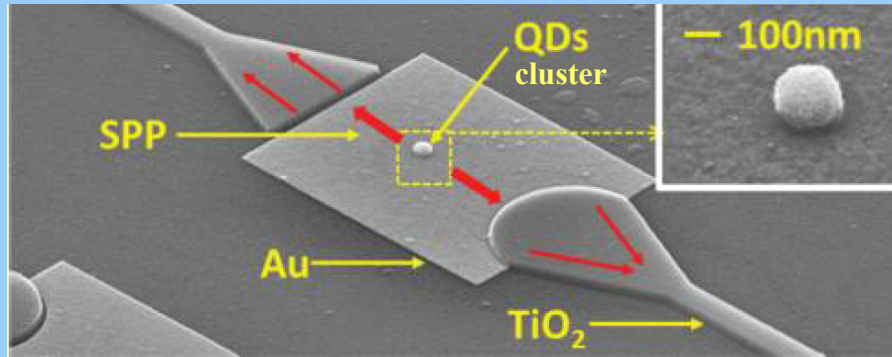


Lossless ideal metal

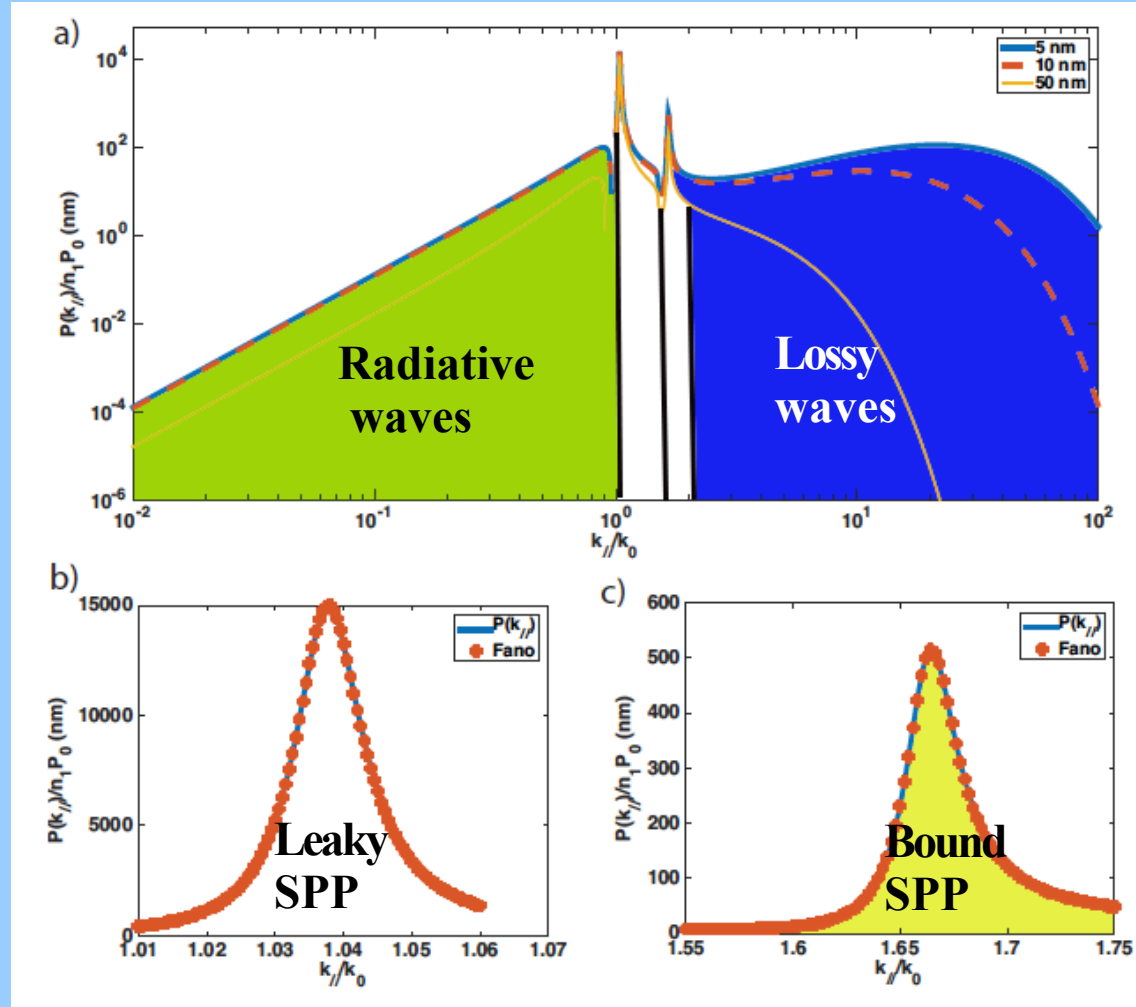
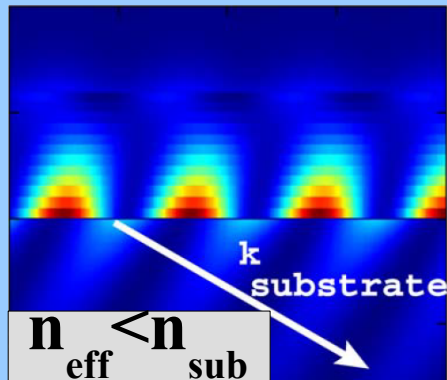
$$\frac{\Gamma_{\perp}(d)}{n_1 \Gamma_0} = \frac{3\pi}{n_1^3} \frac{n_{SPP}^5}{\varepsilon_1 - \varepsilon_2} |\varepsilon_2|^{1/2} e^{-2(\varepsilon_1/|\varepsilon_2|)^{1/2} k_{SPP} d}$$

Γ_{SPP} does not depend on losses (coupling to a mode then propagates with or without losses)
High Purcell factor

Overcoming losses – hybrid plateform



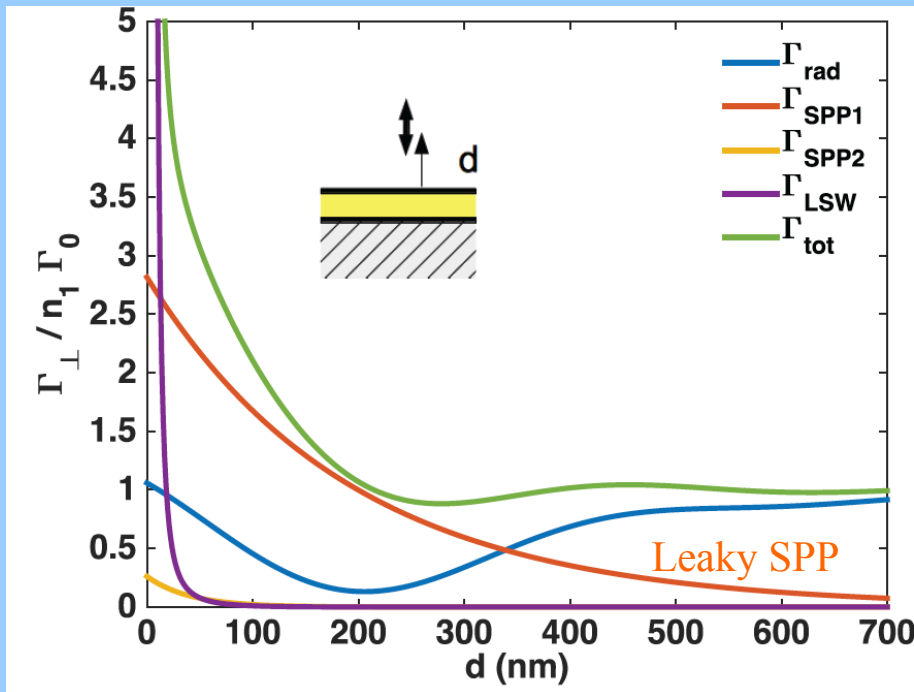
Thin film – leaky SPP



(Fano profile)

Decay channels

Relaxation channels

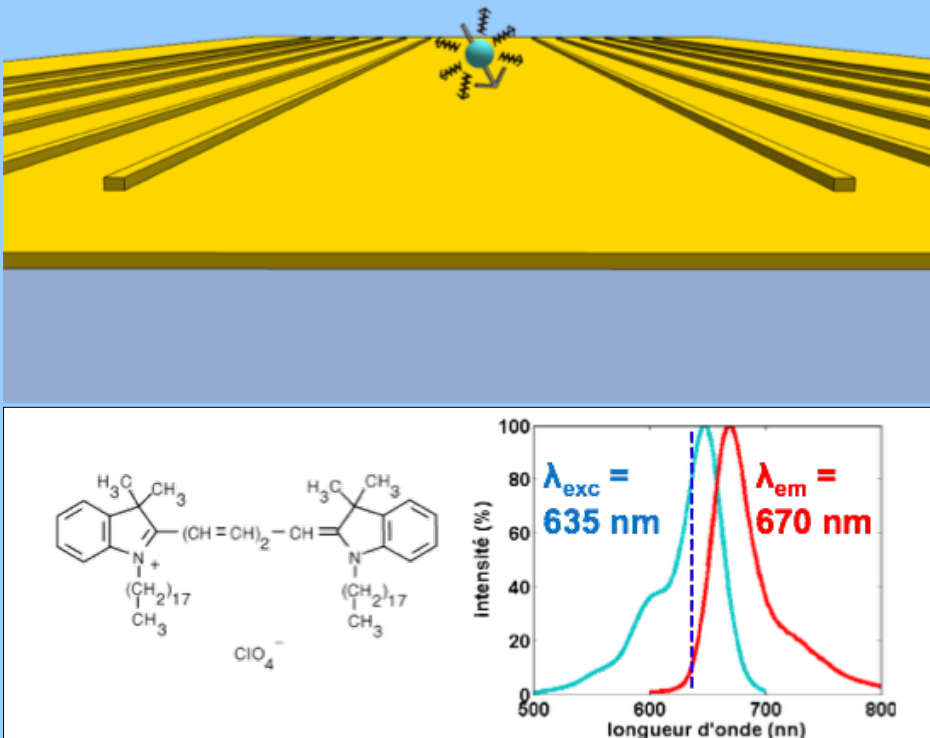


$$L_{SPP} = \frac{1}{\alpha_{abs}} + \frac{1}{\alpha_{leak}}$$

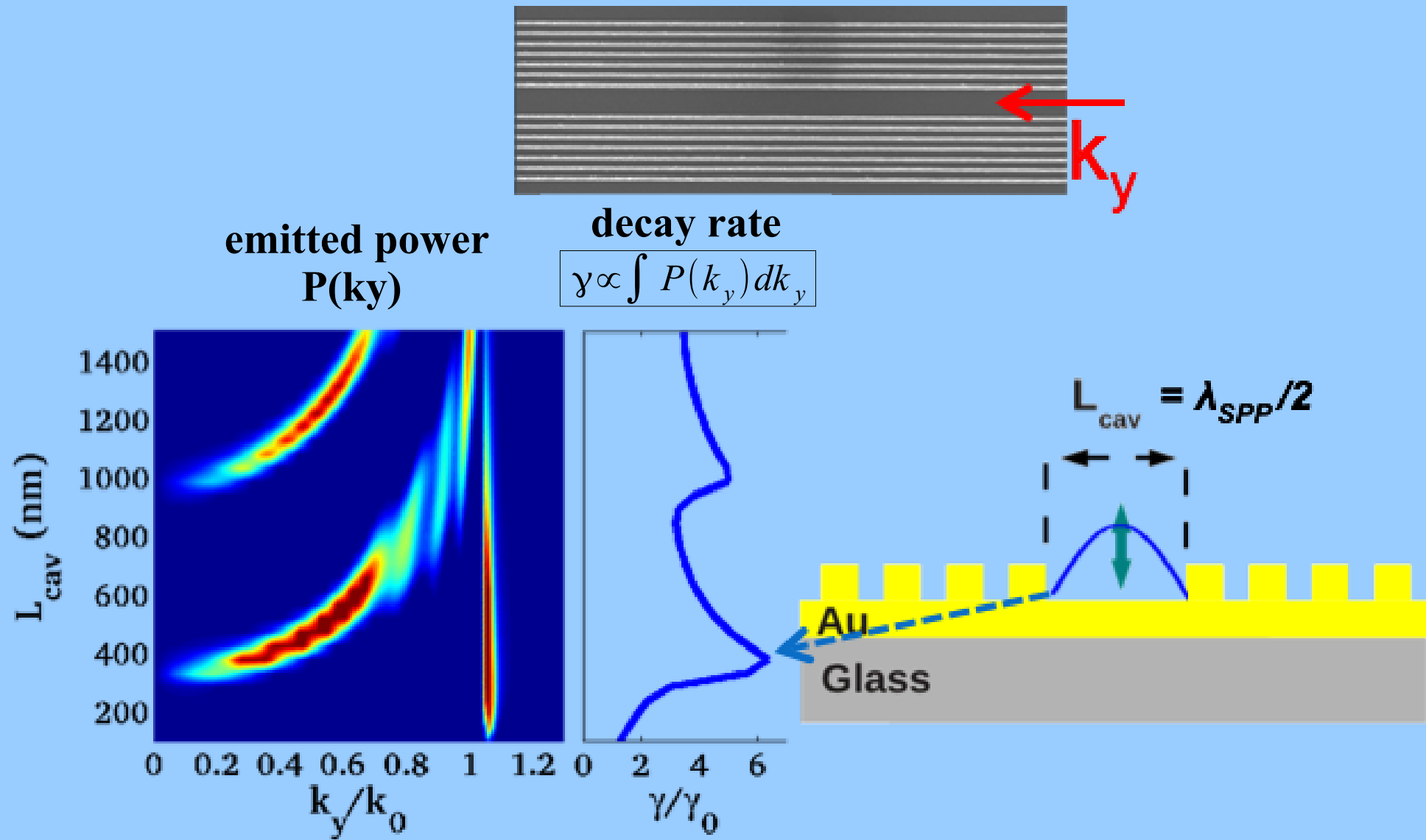
$t_{\text{Au}} \sim 50 \text{ nm} \Rightarrow 50 \% \text{ leakage}$
Detectable using high NA (SPCE)

	Q	L_{eff} (nm)	$\delta/2$ (nm)	n_g	F_p
leaky	85	159	193	0.92	3.02
bound	57	27	76	0.57	5.1

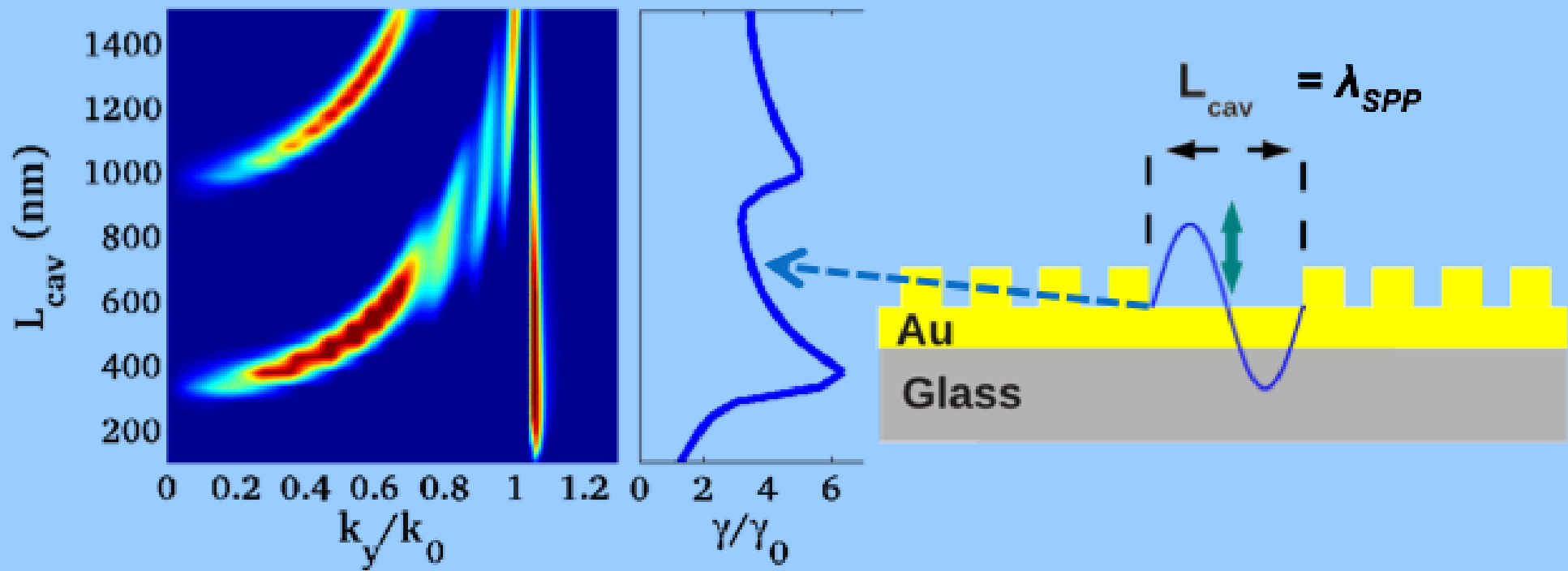
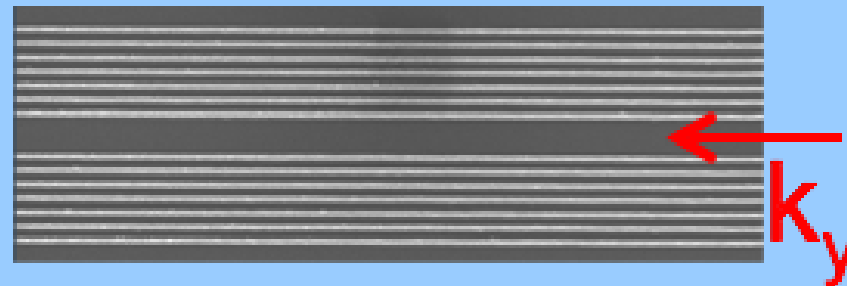
In plane SPP cavity



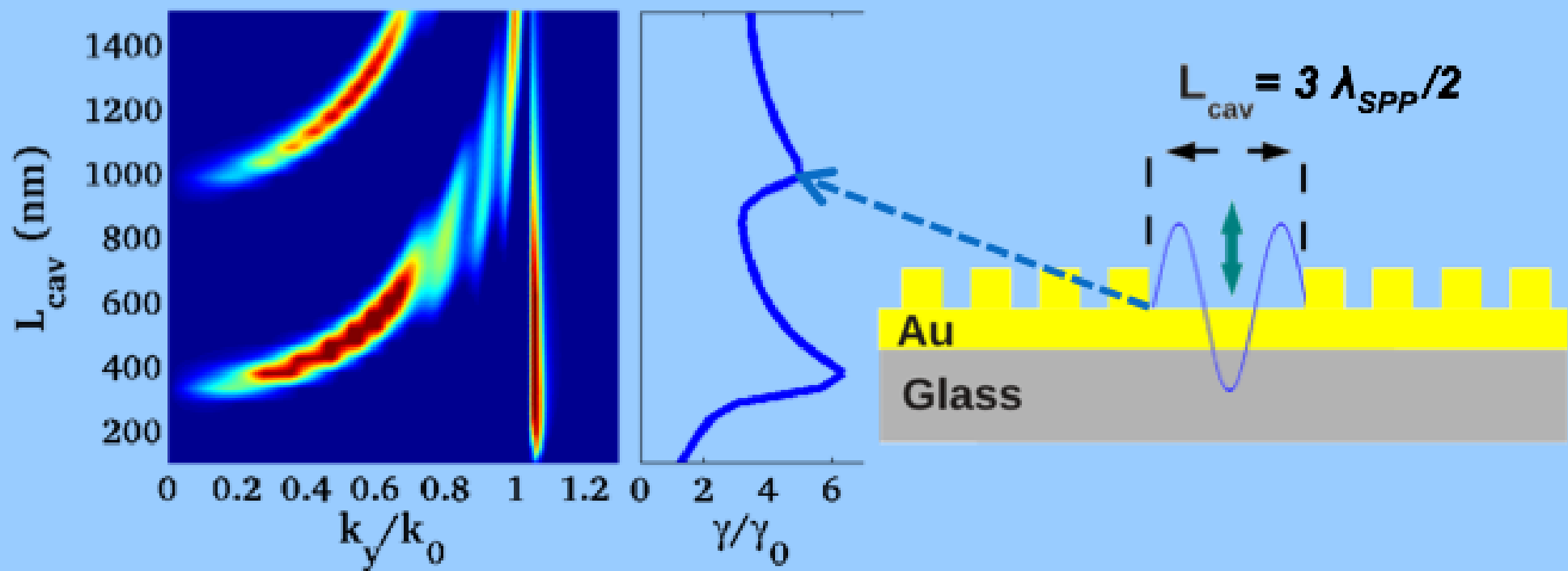
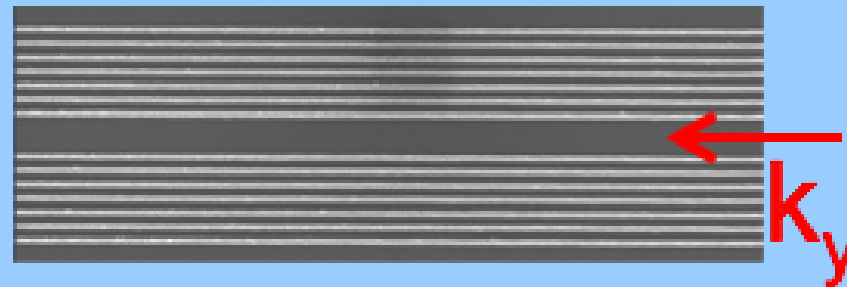
In plane SPP cavity



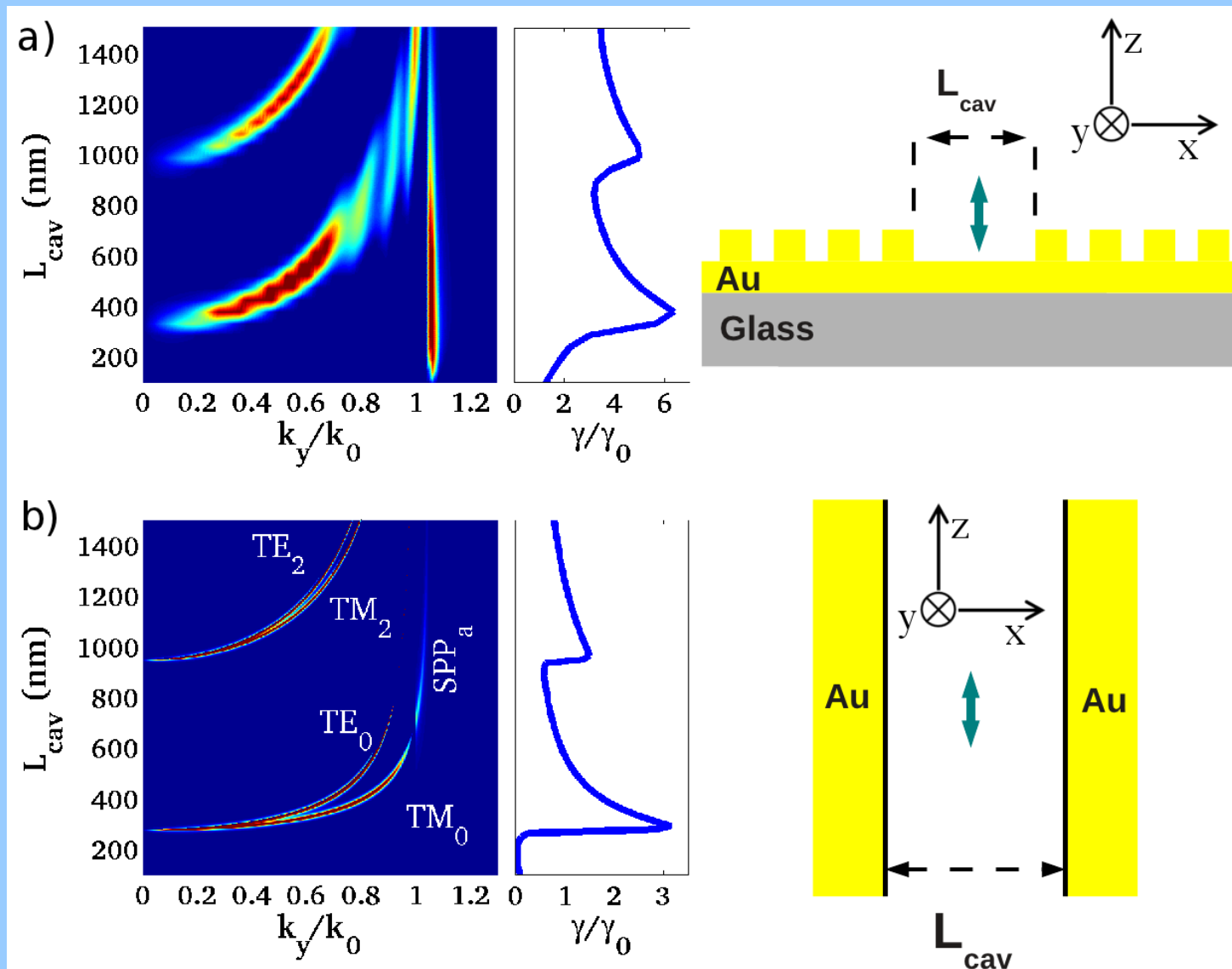
In plane SPP cavity



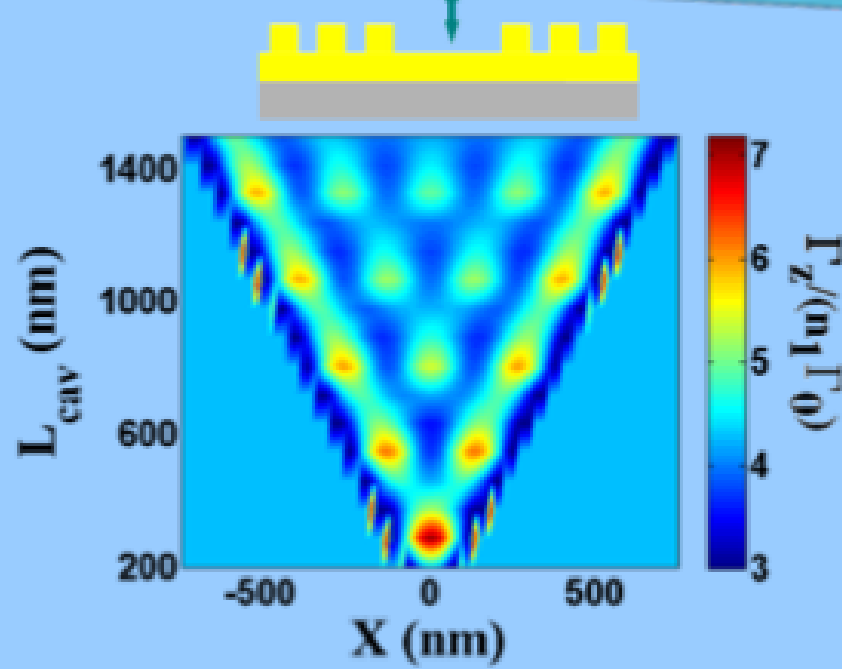
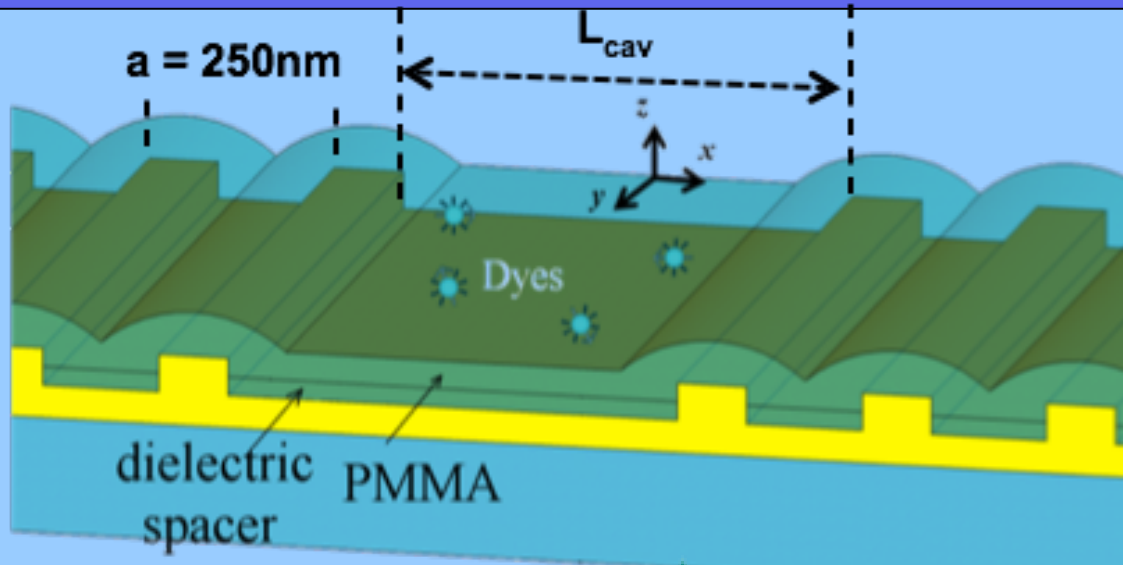
In plane SPP cavity



Comparison between planar and bulk cavities

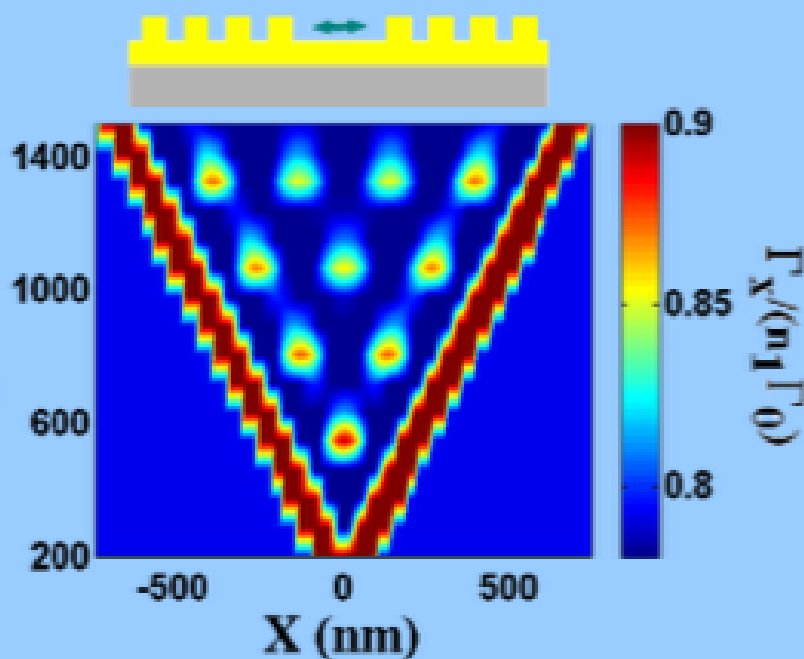


In plane SPP cavity

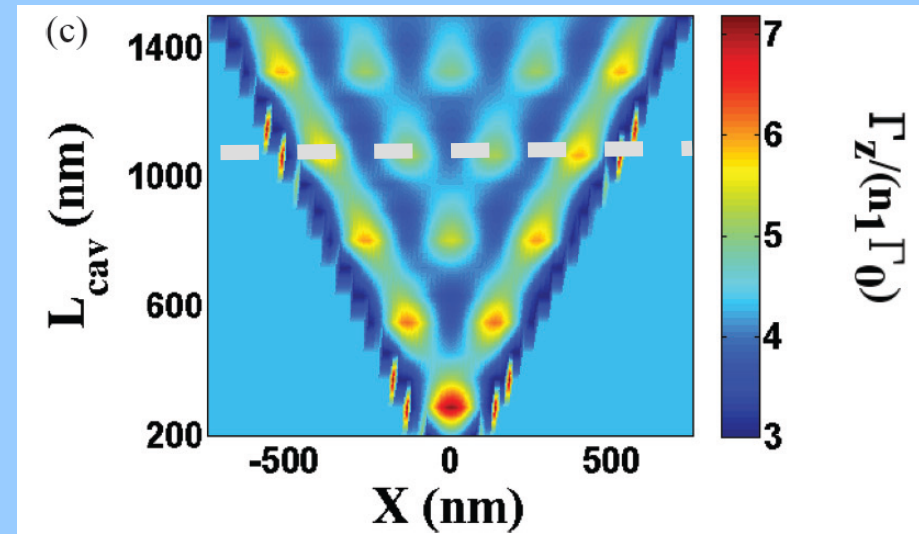
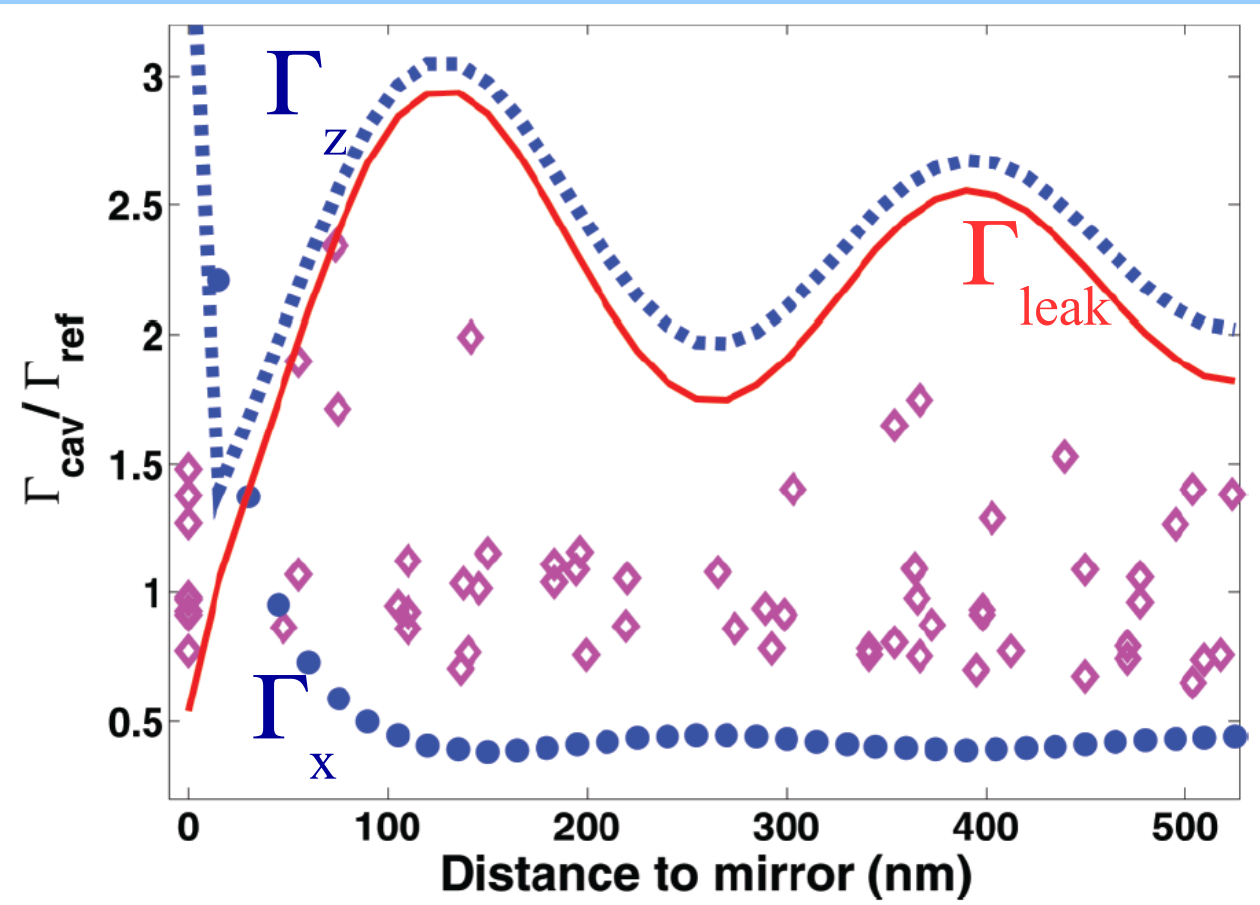


Decay rate depends on

- the cavity length
- the molecule position
- the molecule orientation



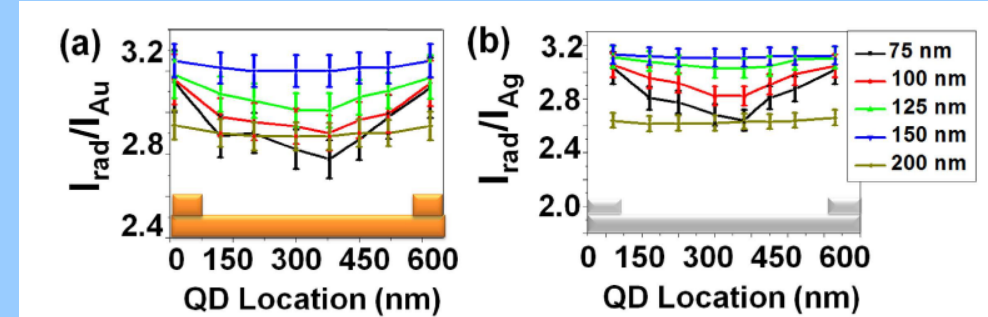
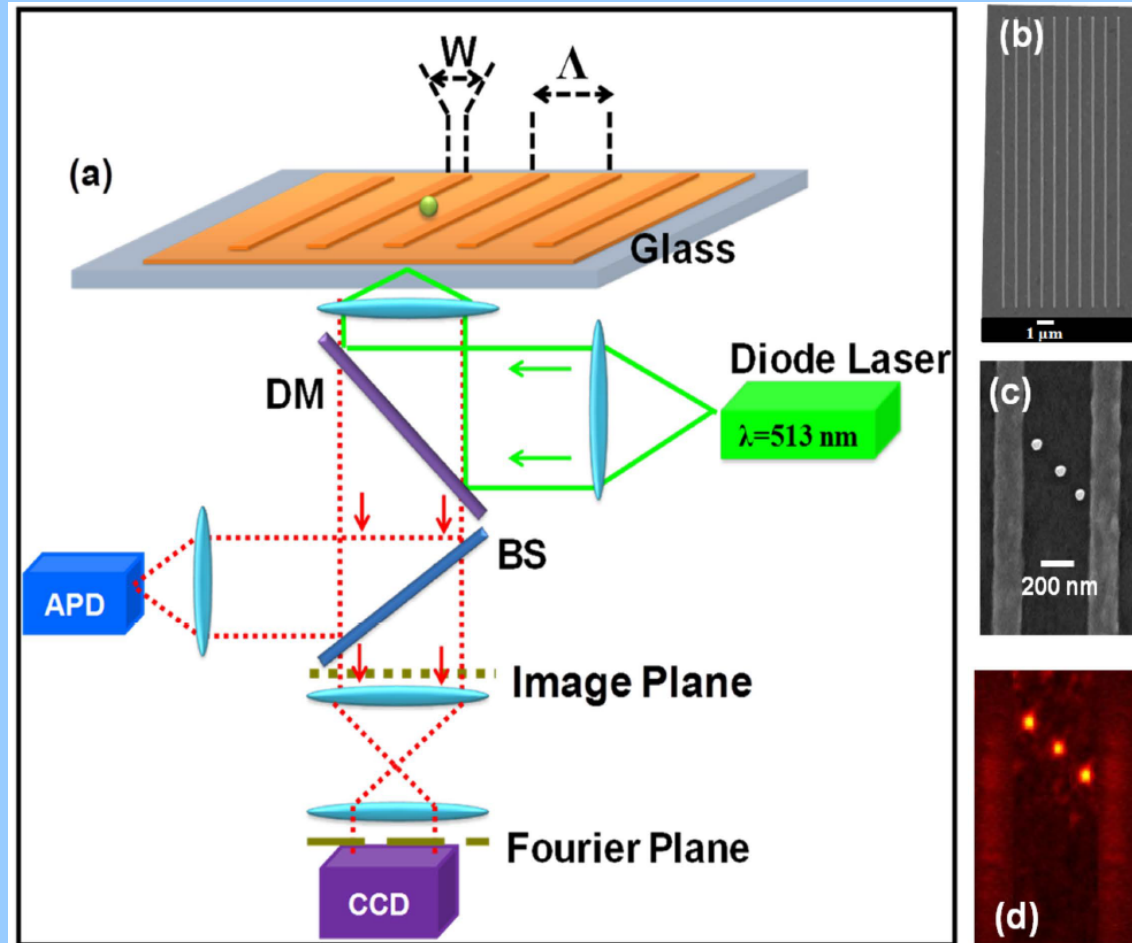
Single cavity ($L_{\text{cav}} = 2 \lambda_{\text{SPP}} = 1,1 \mu\text{m}$)



$$F_p \sim 7 \left(\frac{\lambda_{\text{SPP}}}{2} \text{ cavity} \right) \quad \frac{\Gamma_{\text{leak}}}{\Gamma_{\text{tot}}} \approx 0.8$$

Extraction efficiency
(leakage into the substrate)

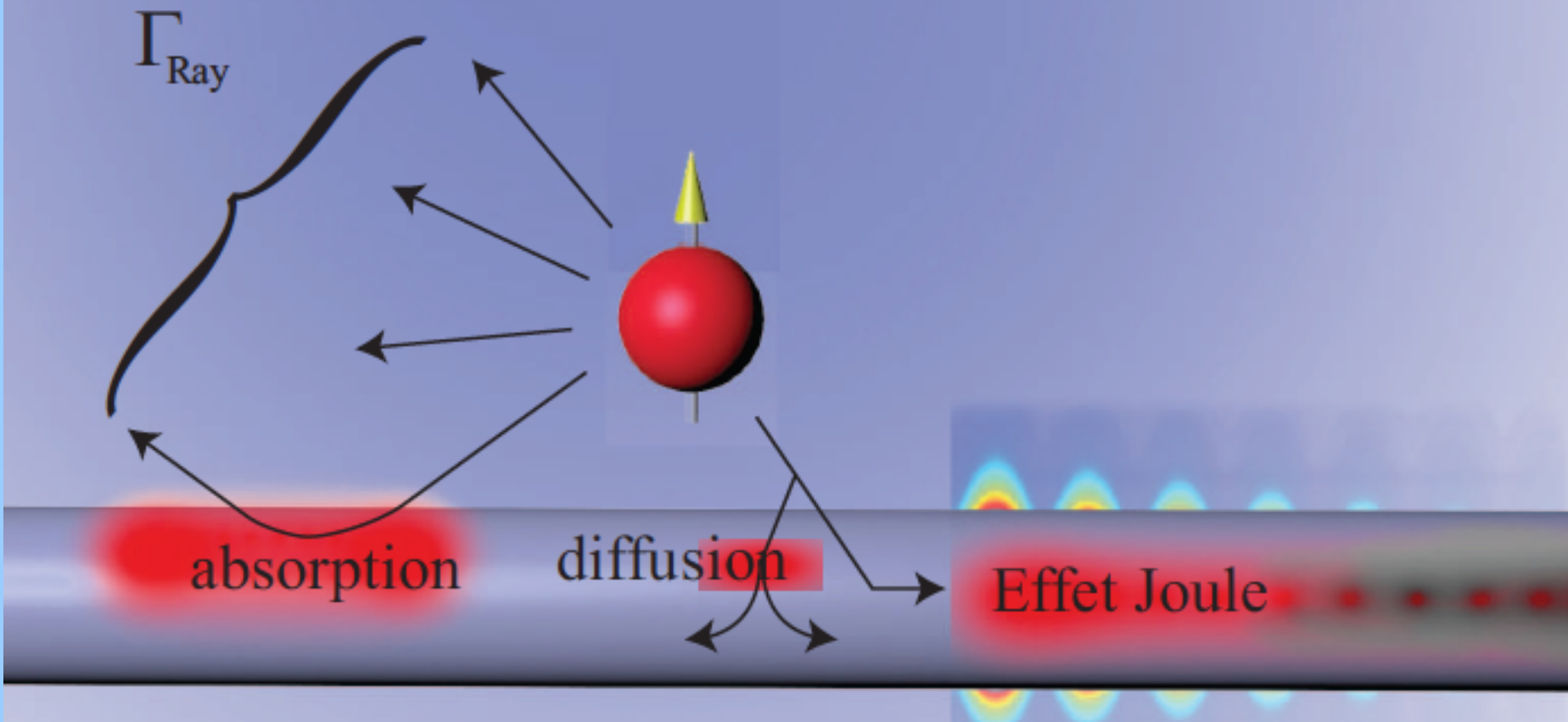
Grating decoupler



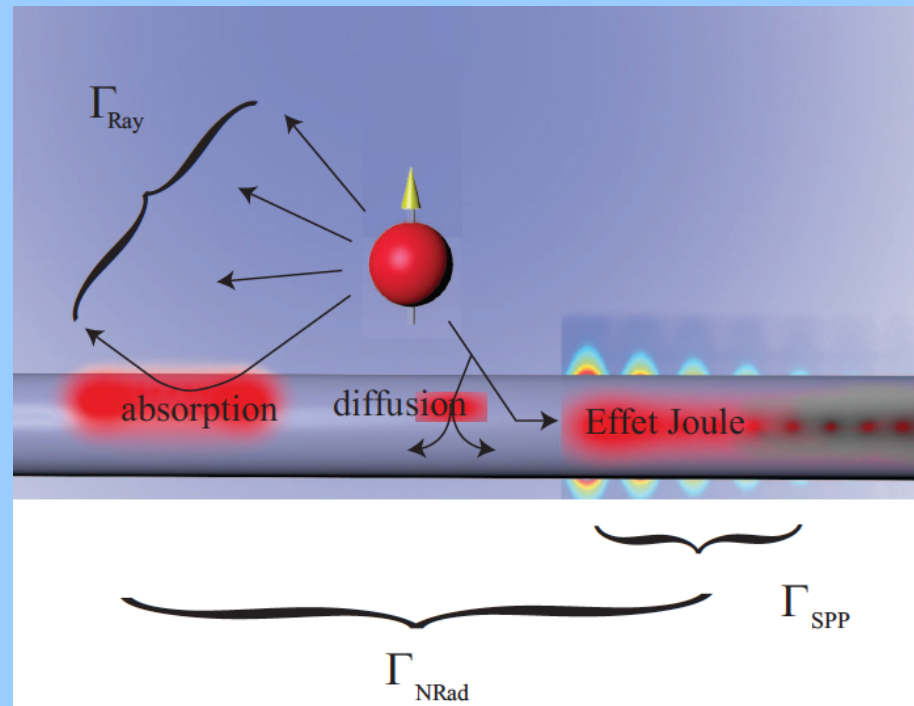
Fluorescence enhancement
(independent of position)

Extraction efficiency

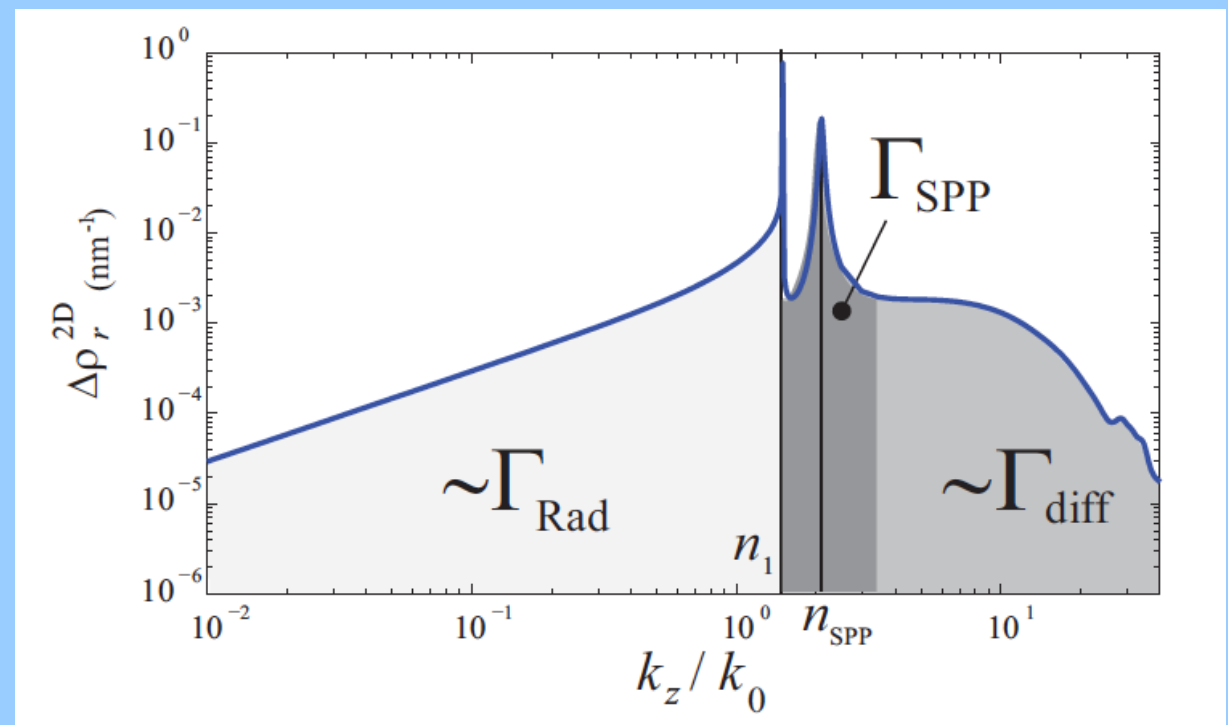
Nanowire



Decay channels

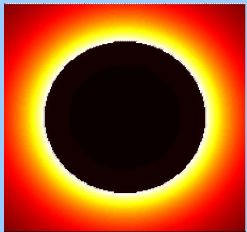


$$2D-DOS$$
$$\rho^{2D}(k_z) = \frac{-2k_z}{\pi} \operatorname{Im} \operatorname{Tr} [\epsilon \mathbf{G}^{2D}(k_z)]$$



Purcell and β factors

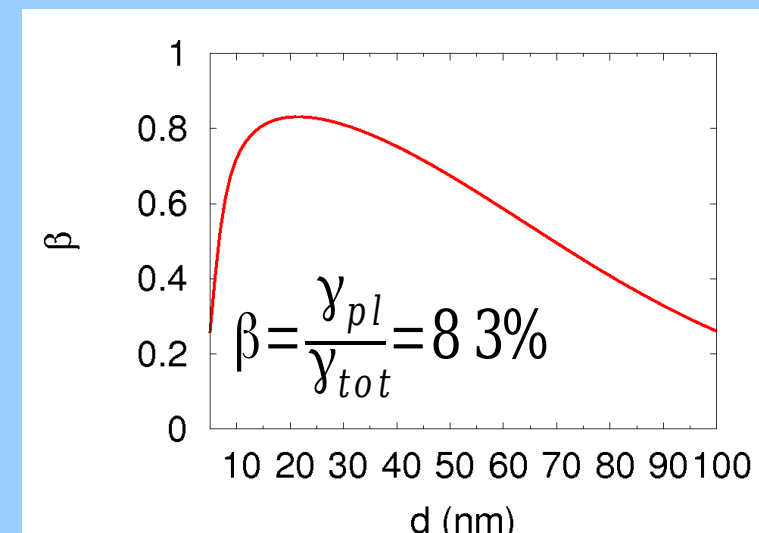
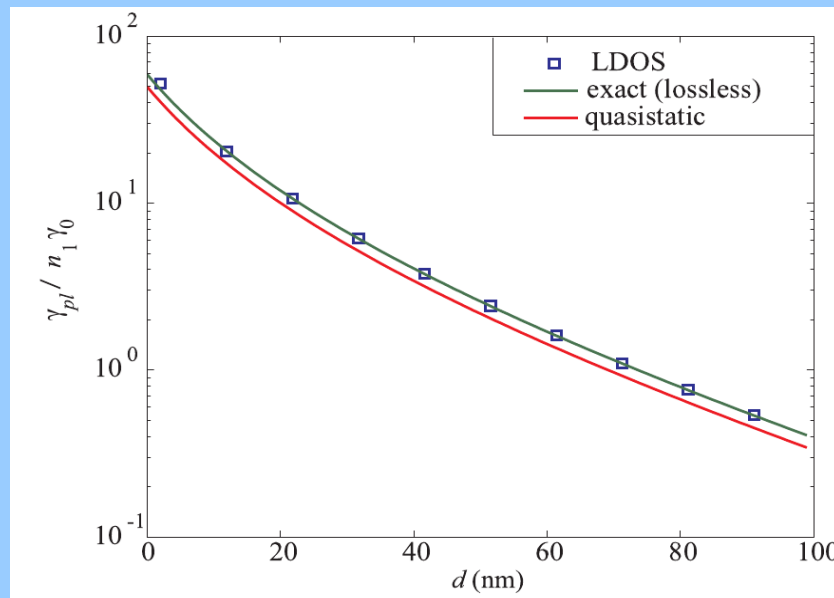
Overlap with the guided mode



$$\frac{\Gamma_{spp}}{\Gamma_0} = \frac{3}{8 n_{eff}} \left(\frac{\lambda}{n} \right)^2 \frac{\rho^{2D}(k_{spp})}{L_{spp}}$$

propagation in the 3rd direction

High coupling efficiency (β -factor)



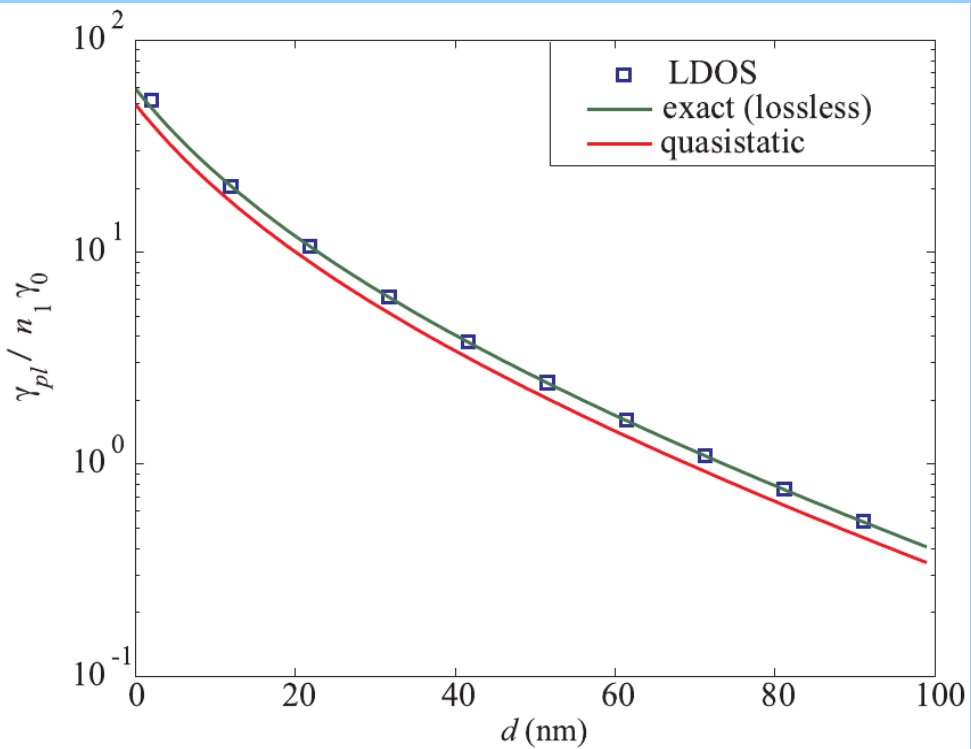
Effect of Joule losses

Exact lossless case

$$\frac{\Gamma_{spp}}{\Gamma_0} = \frac{3\pi C}{k_0^2} \frac{E_u(d) E_u^*(d)}{\int_{A_\infty} (\mathbf{E} \times \mathbf{H}^*). \mathbf{z} dA}$$

2D-LDOS (lossy)

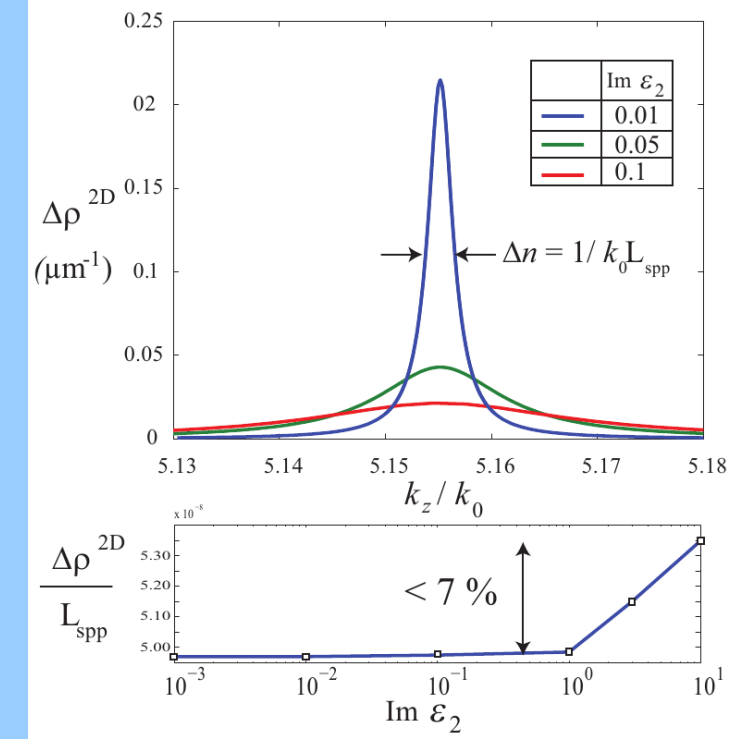
$$\frac{\Gamma_{spp}}{\Gamma_0} = \frac{3}{8n_{eff}} \left(\frac{\lambda}{n}\right)^2 \frac{\rho^{2D}(k_{spp})}{L_{spp}}$$



Nb of modes

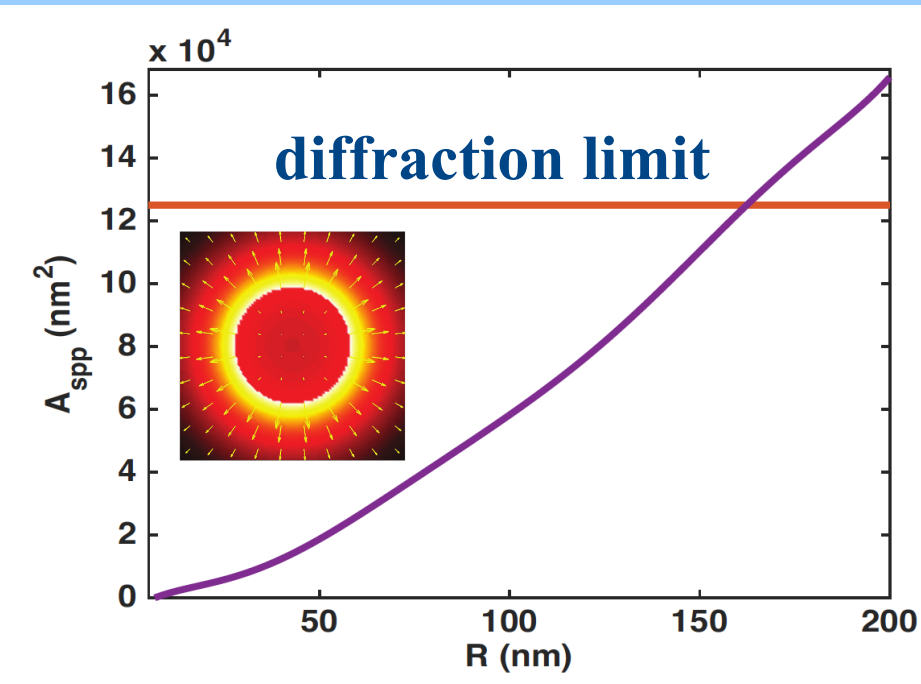
$$N \propto \int dk_z \rho^{2D}(k_z) \propto \frac{\rho^{2D}(k_{spp})}{L_{spp}}$$

independent
on losses

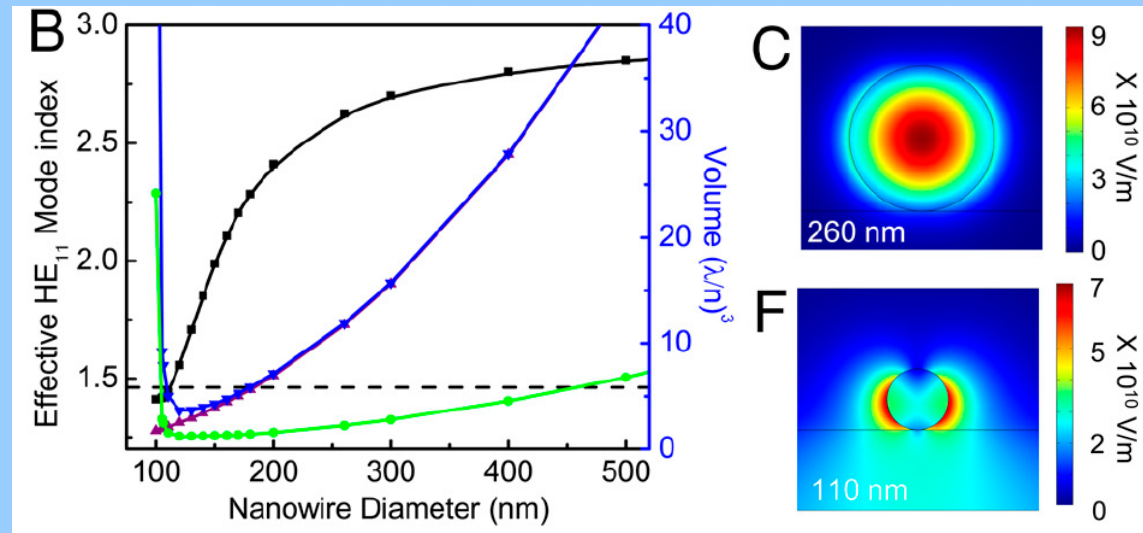


Mode confinement

SPP nanowire



Photonic waveguide

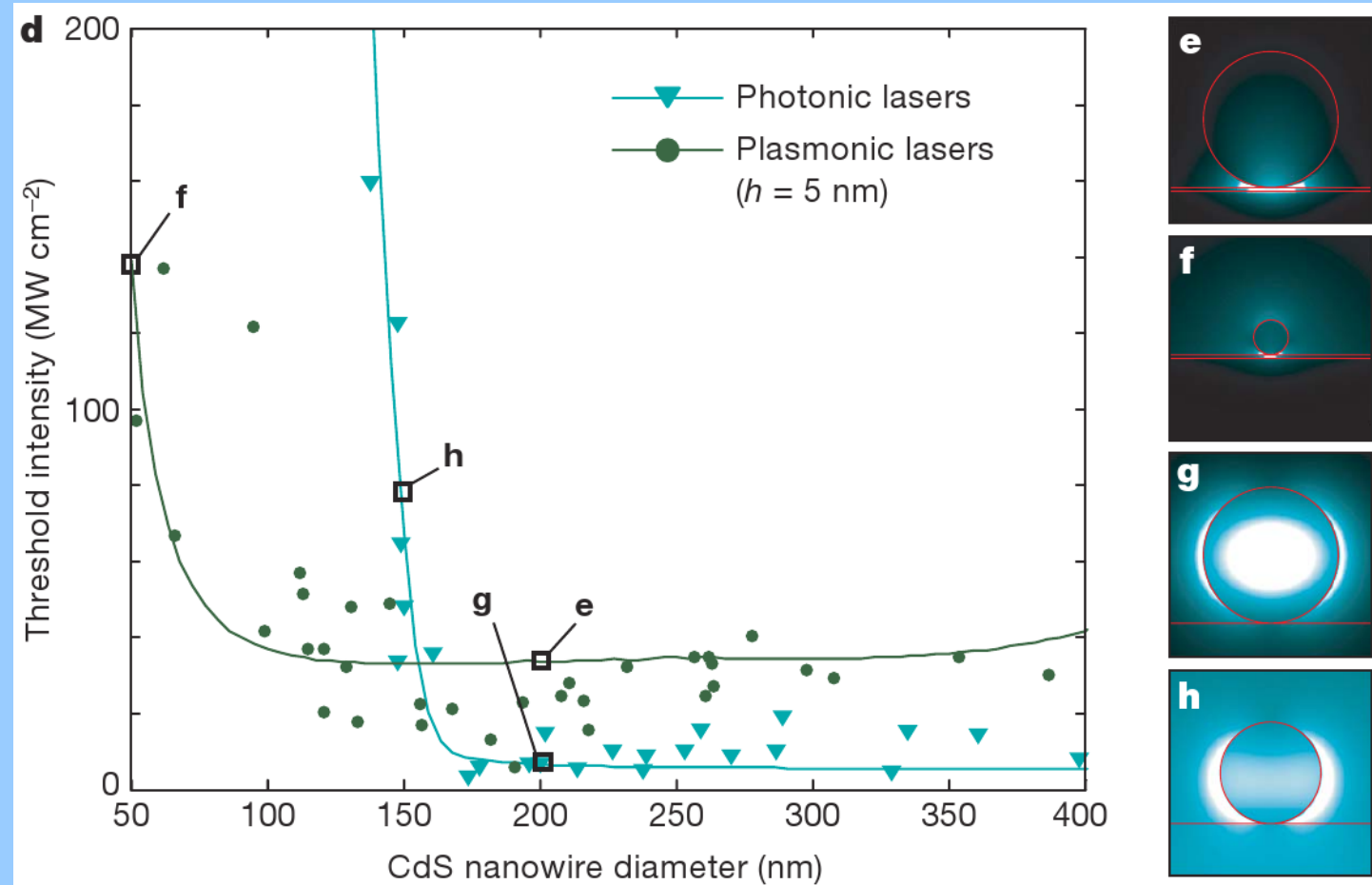
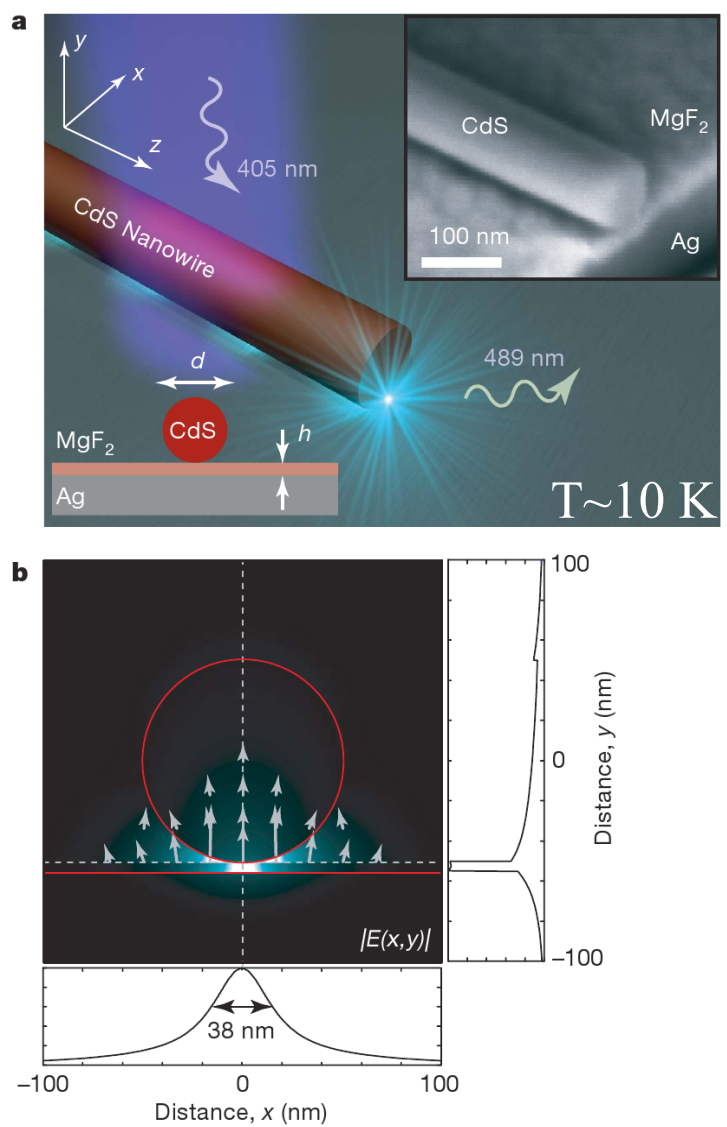


Agarwal *et al*, PNAS **108**, 10050 (2011)

$$\frac{\Gamma_{spp}}{\Gamma_0} = \frac{3}{8 n_{eff}} \left(\frac{\lambda}{n} \right)^2 \frac{\rho^{2D}(k_{spp})}{L_{spp}}$$

$$\frac{\Gamma_{guided}}{n_1 \Gamma_0} = \frac{3 n_g}{4 \pi n_1} \frac{(\lambda/n_1)^2}{A_{eff}}$$

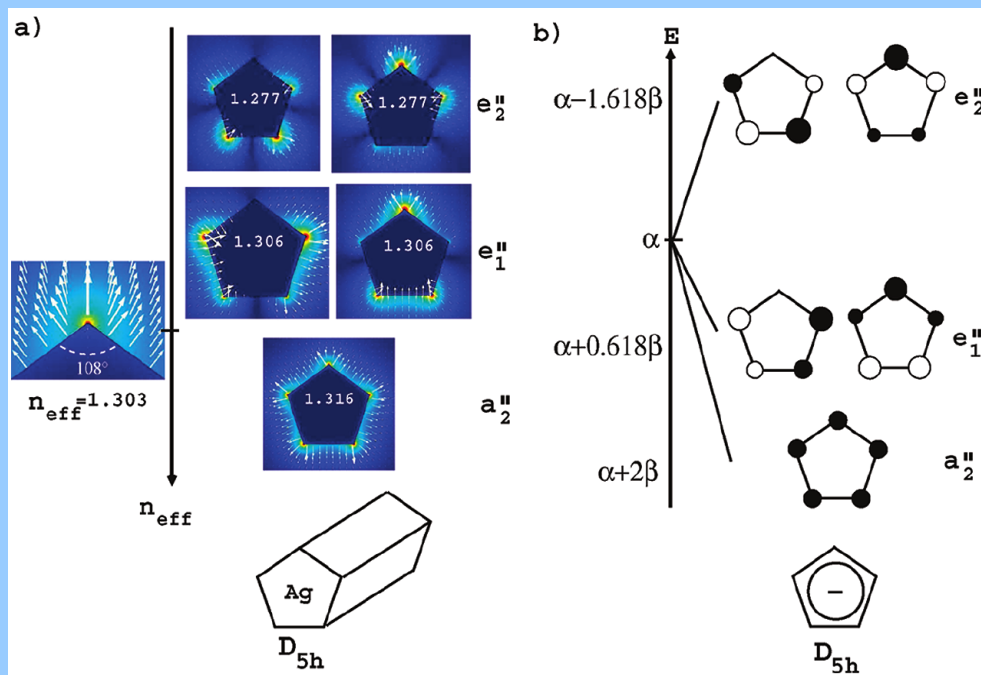
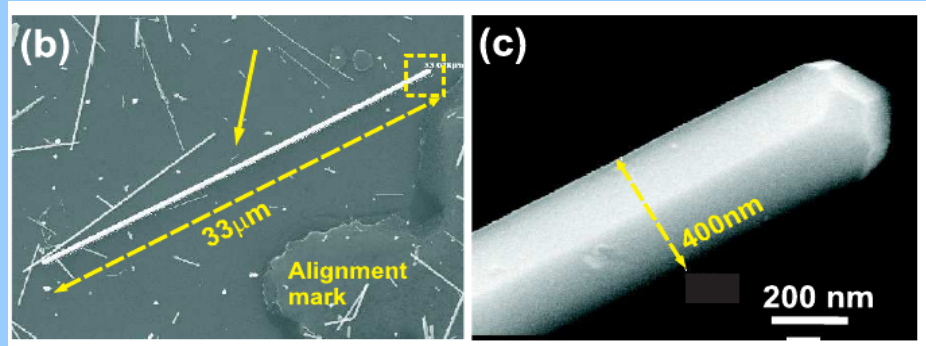
Plasmonic laser



Plasmon laser at deep subwavelength scale

Oulton *et al*, Nature 461(2009) 629 ,

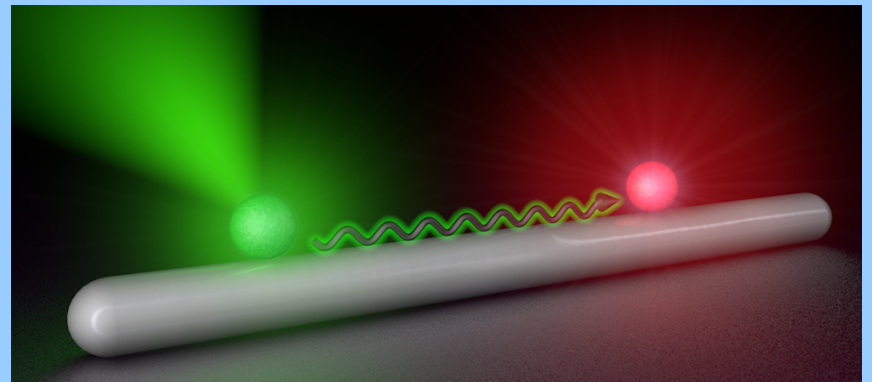
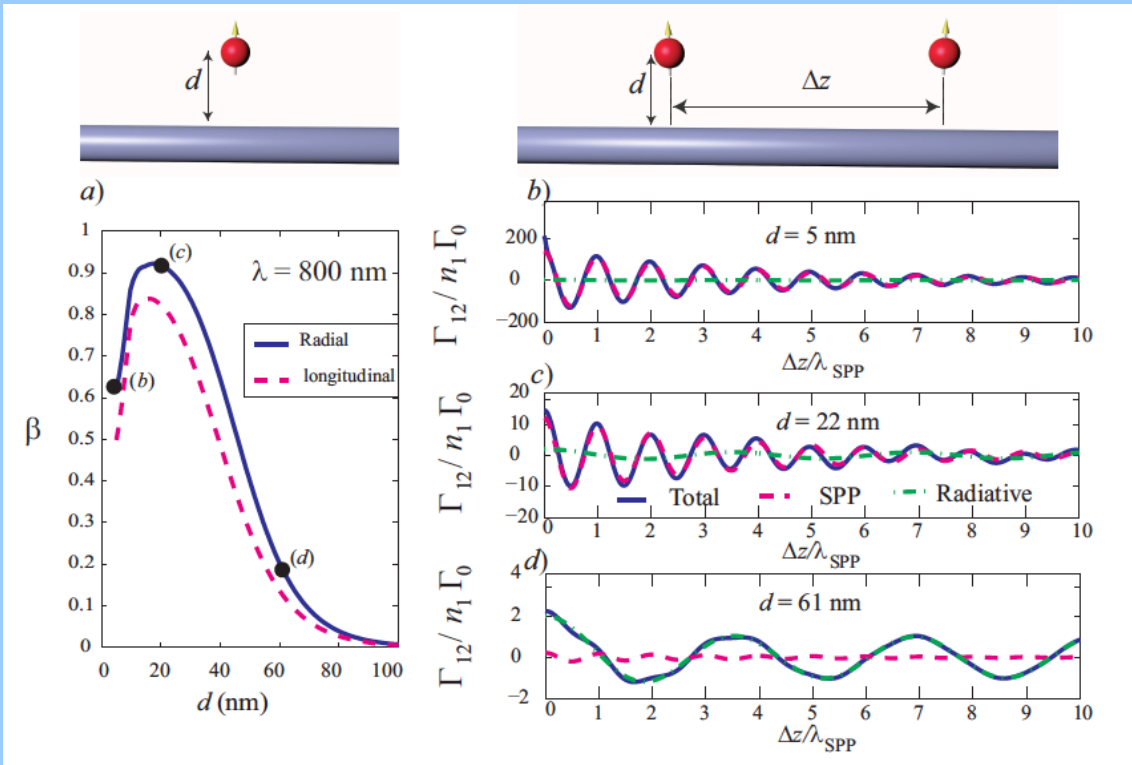
Crystalline Ag wire



High modal confinement in the corners
=> high Purcell factor

Lower losses (crystalline/amorphous metal)
=> high β factor

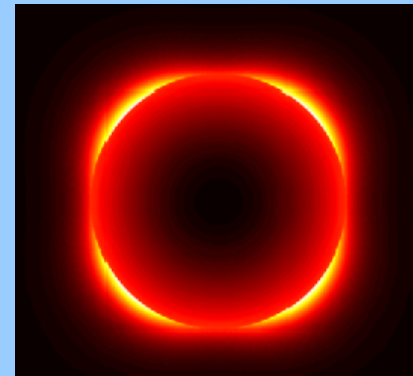
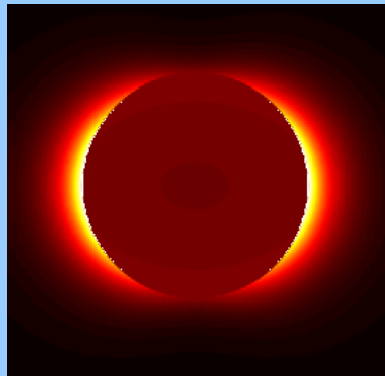
Resonant energy transfer



de Torres, Wenger *et al*,
ACS Phot. 10, 3968 (2016)

Coupling of a dipolar emitter into
one-dimensional surface plasmon, Barthes *et al*,
Sci. Rep. 3, 2734 (2013)

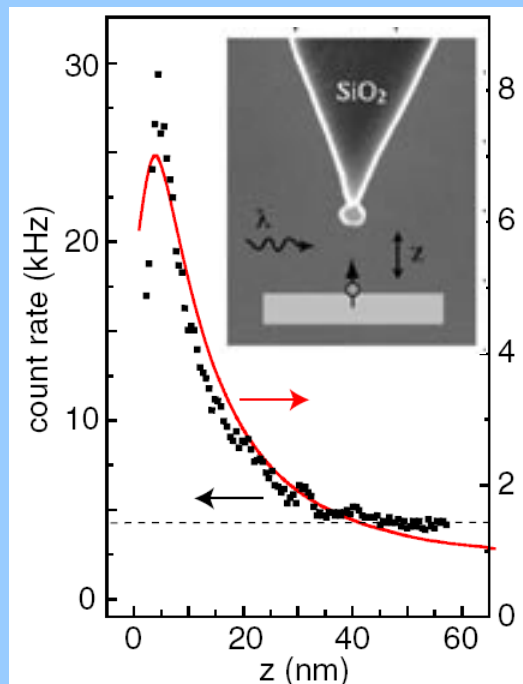
Localized plasmon (3D)-Purcell factor



Surface enhanced spectroscopies

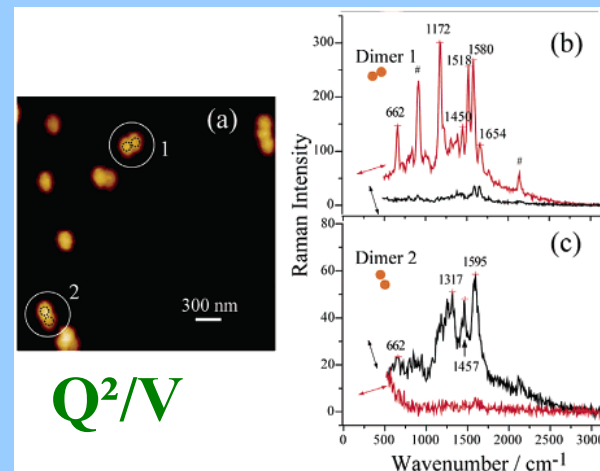
Surface enhanced spectroscopie

Raman (SERS), Fluorescence



P. Anger, L. Novotny
PRL **96**, 113002 (2006)

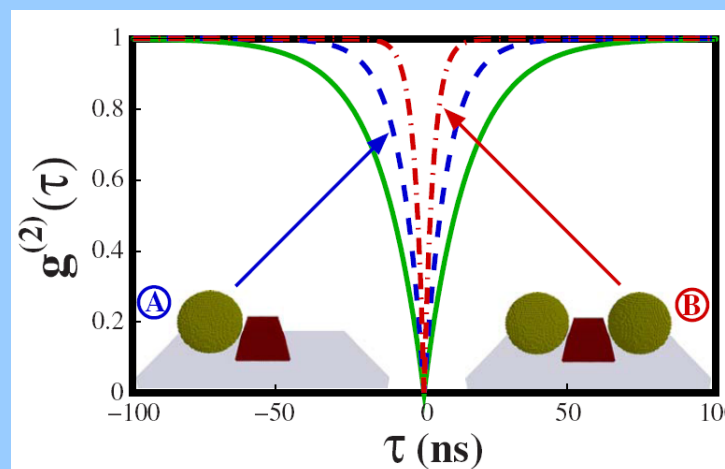
Coupling
Q/V



Imura et. al.
Nano Lett., 6 2006)

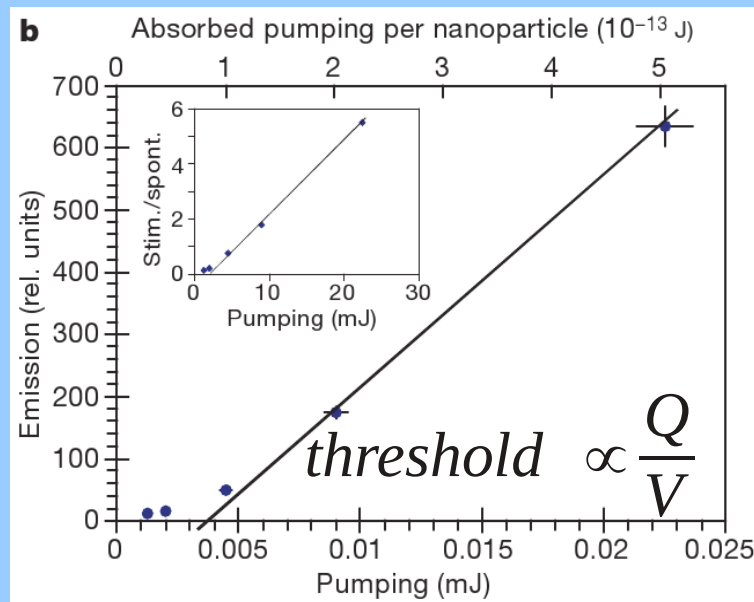
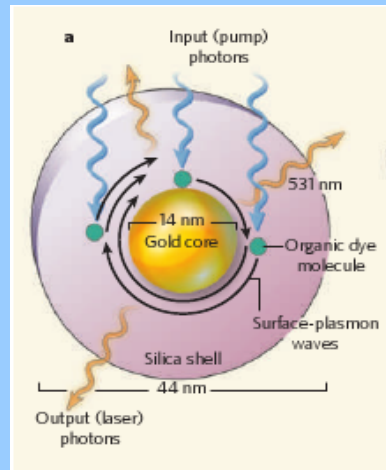
Maier
Opt. Exp 4, 1957 (2006)

Control of photons antibunching:

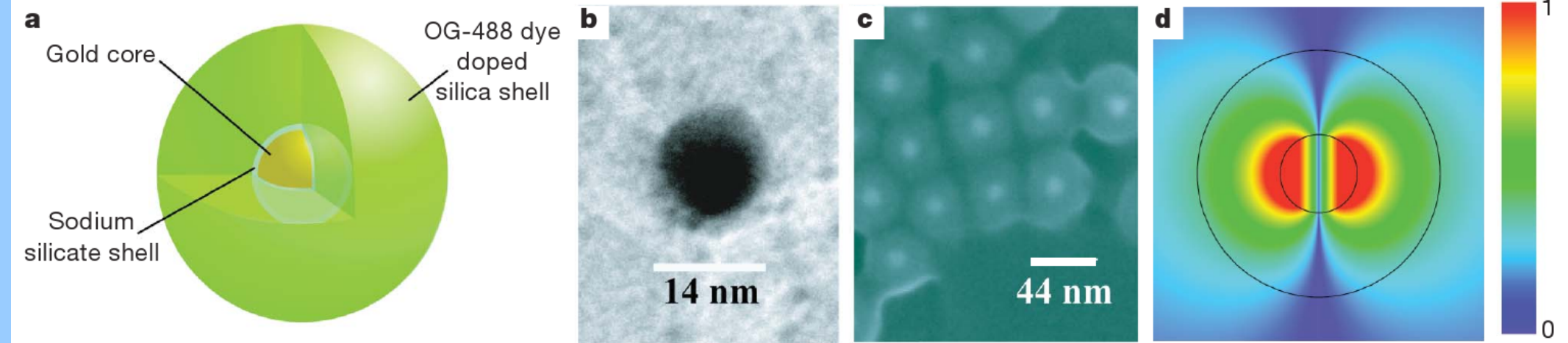


S. Schietinger, O. Benson
Nano Lett. **9**, 1694 (2009)
Marty, Girard, Colas des Francs
PRB **82**, 081403R(2010)

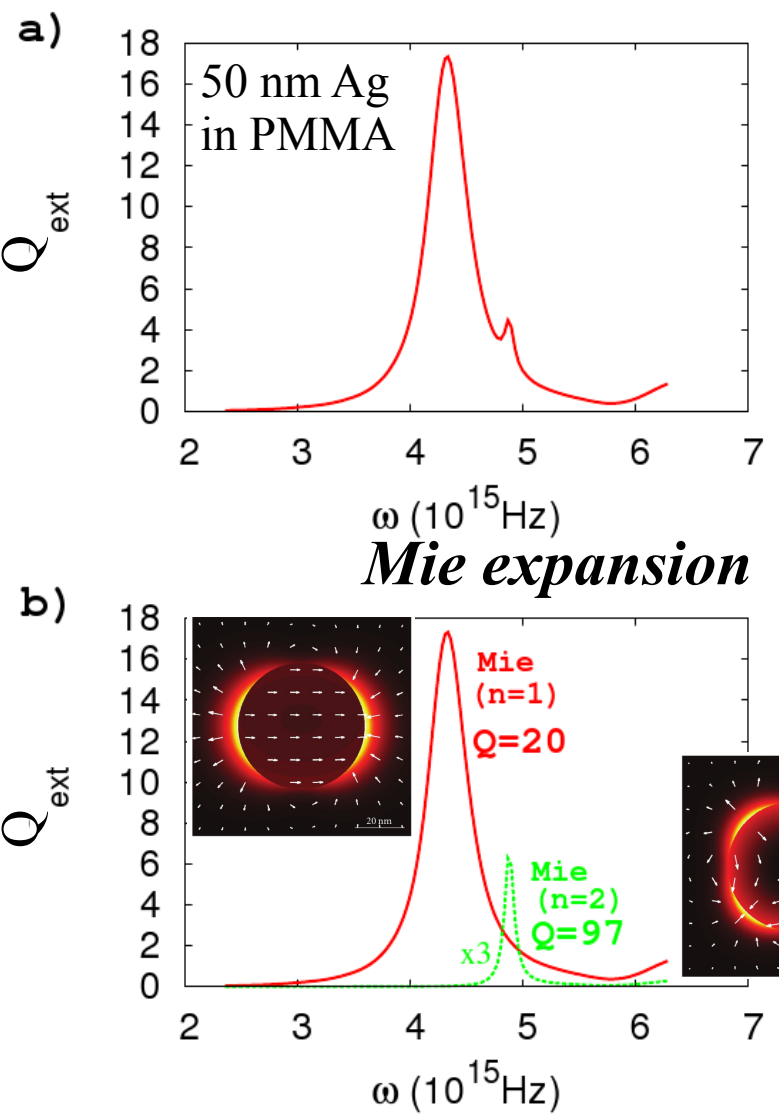
Perspectives : plasmon nanolaser (SPASER)



localized,
coherent
and ultra-fast
nanosource



Quality factor of localized SPP



$$\mathbf{p}^{(1)}(\omega) = 4\pi\epsilon_0\alpha_1(\omega)\mathbf{E}_0$$

$$\alpha_1(\omega) = \frac{\epsilon_m(\omega) - 1}{\epsilon_m(\omega) + 2} R^3$$

*Quasi-static
approx*

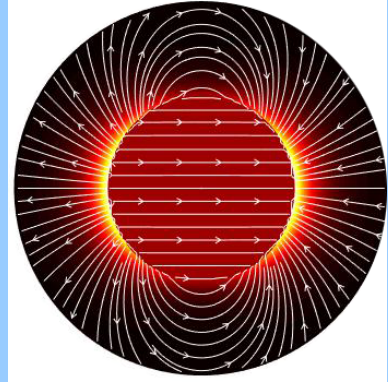
$$\begin{aligned} \epsilon_m &= 1 - \frac{\omega_p^2}{\omega^2 + i\kappa_{abs}\omega} \\ \alpha_1^{eff}(\omega) &\sim \frac{\omega_1}{2(\omega_1 - \omega) - i\kappa_1} R^3 \\ \kappa_1 &= \kappa_{abs} + \frac{2(k_1 R)^3 \omega_1}{3} \end{aligned}$$

Joule losses Radiative leakage

Quality factor

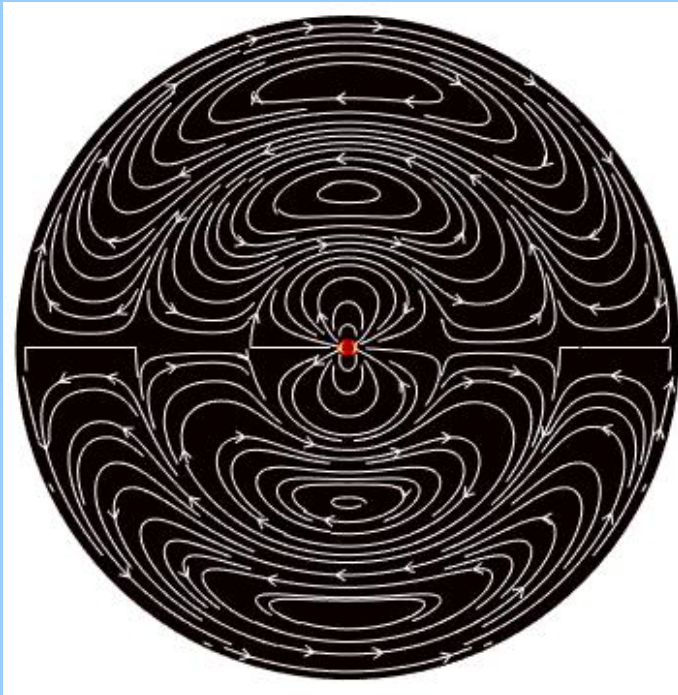
$$Q_1 = \frac{\omega_1}{K_1}$$

Mode volume definition

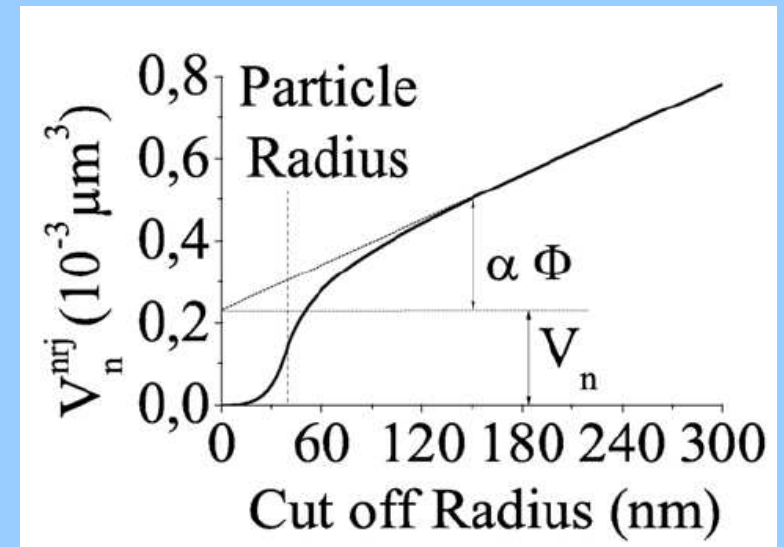


Near field confinement

$$V_n^{nrj} = \frac{\int U_n(\mathbf{r}) d\mathbf{r}}{\max[\varepsilon_0 \varepsilon_1 |E_n(\mathbf{r})|^2]} ,$$
$$U_n(\mathbf{r}) = \frac{\partial [\omega \varepsilon_0 \varepsilon(\mathbf{r}, \omega)]}{\partial \omega} |E_n(\mathbf{r})|^2 + \mu_0 |H_n(\mathbf{r})|^2$$



Far field scattering



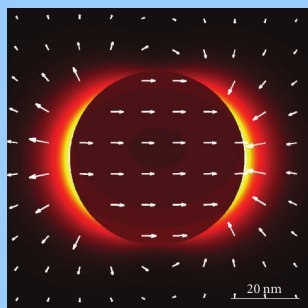
Mode volume - quasi-static approximation

Dipolar LSP response

$$\frac{\gamma_1^\perp}{\gamma_0} \sim \frac{6}{k^3 z_0^6} \text{Im}(\alpha_1)$$

$$\frac{\langle \Gamma_1 \rangle}{\Gamma_0} = \frac{\Gamma_1^\perp + 2\Gamma_1^\parallel}{3\Gamma_0} \sim \frac{3}{4\pi^2} \lambda_1^3 \frac{1}{2\pi R^3} Q_1$$

$$= \frac{3}{4\pi^2} \lambda_1^3 \frac{Q_1}{V_1}$$



$$V_1 = 1.5 V_{part}$$

$$V_{part} = \frac{4}{3} \pi R^3$$

n^{th} LSP response

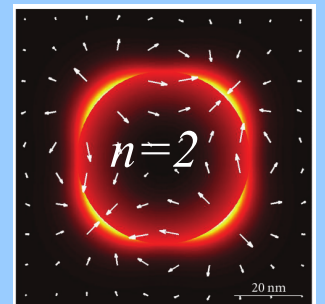
$$\mathbf{p}^{(n)} = \frac{4\pi\epsilon_0}{(2n-1)!!} \alpha_n \nabla^{n-1} \mathbf{E}_0$$

$$\alpha_n = \frac{n(\epsilon_m - 1)}{n\epsilon_m + (n+1)} R^{(2n+1)}$$

$$\frac{\Gamma_n}{\Gamma_0} = (2n+1) F_p$$

degenerescence

$$V_n = \frac{3}{n+1} V_{part}$$



Mie plasmons: quality factors, effective volumes and coupling strength to a dipolar emitter
 Colas des Francs, Derom, Vincent, Bouhelier, Dereux, Int. J. Optics 2012, 175162 (2012)

Mode confinement – cQED extrapolation

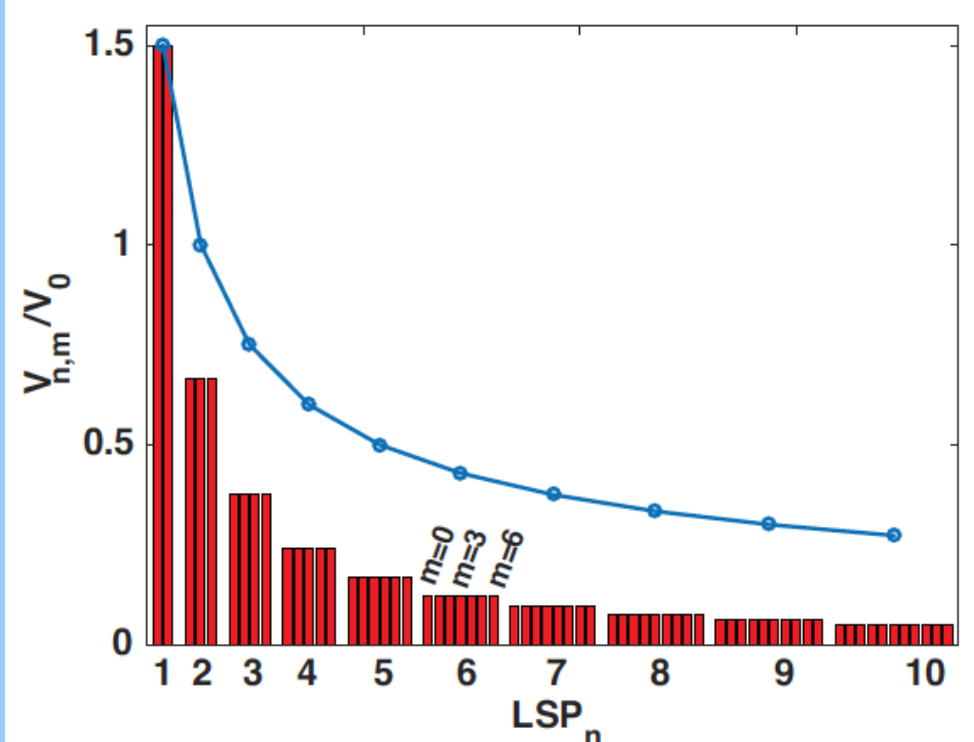
$$V_n^{nrj} = \frac{\int U_n(\mathbf{r}) d\mathbf{r}}{\max[\varepsilon_0 \varepsilon_1 |E_n(\mathbf{r})|^2]} ,$$

$$U_n(\mathbf{r}) = \frac{\partial[\omega \varepsilon_0 \varepsilon(\mathbf{r}, \omega)]}{\partial \omega} |E_n(\mathbf{r})|^2 + \mu_0 |H_n(\mathbf{r})|^2$$

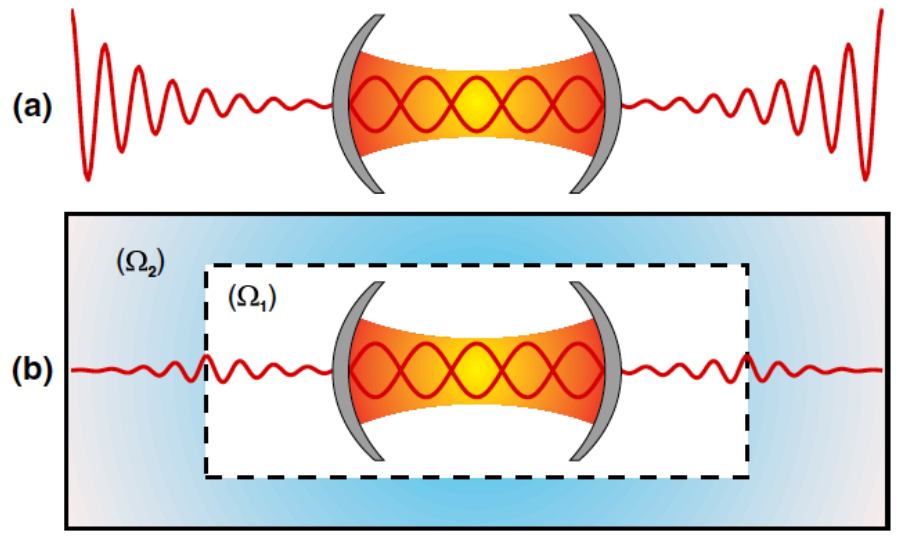
*Quasi-static
approx*

$$V_n^{nrj} = \frac{6}{(n+1)^2} V_{part}$$

*Khurgin and Sun
JOSA B 26, B83 (2009)*



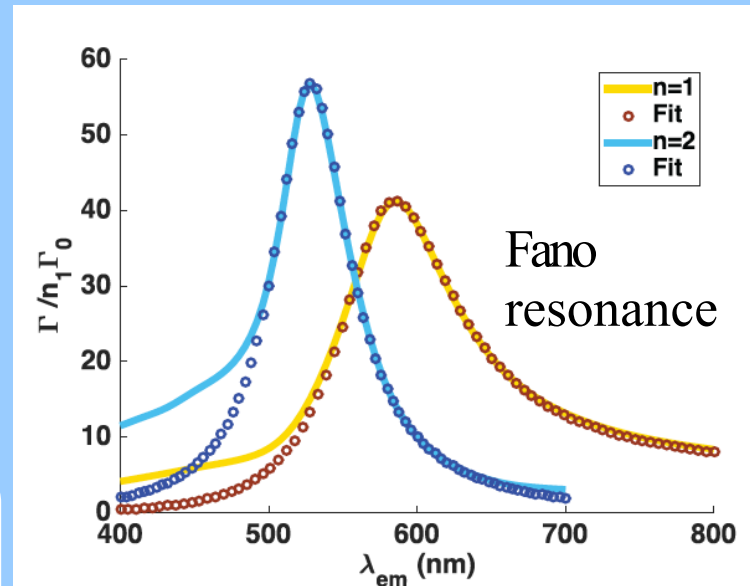
Complex mode volume – the reconciliation



Sauvan, Lalanne
PRL 110 , 237401 (2013)

$$V_n = \frac{\frac{1}{2} \int \tilde{\mathbf{E}}_n \cdot \frac{\partial(\omega \varepsilon_0 \varepsilon)}{\partial \omega} \cdot \tilde{\mathbf{E}}_n - \mu_0 \tilde{\mathbf{H}}_n^2 dr}{\max[\varepsilon_0 \varepsilon_1 |\tilde{\mathbf{E}}_n(\mathbf{r})|^2]}$$

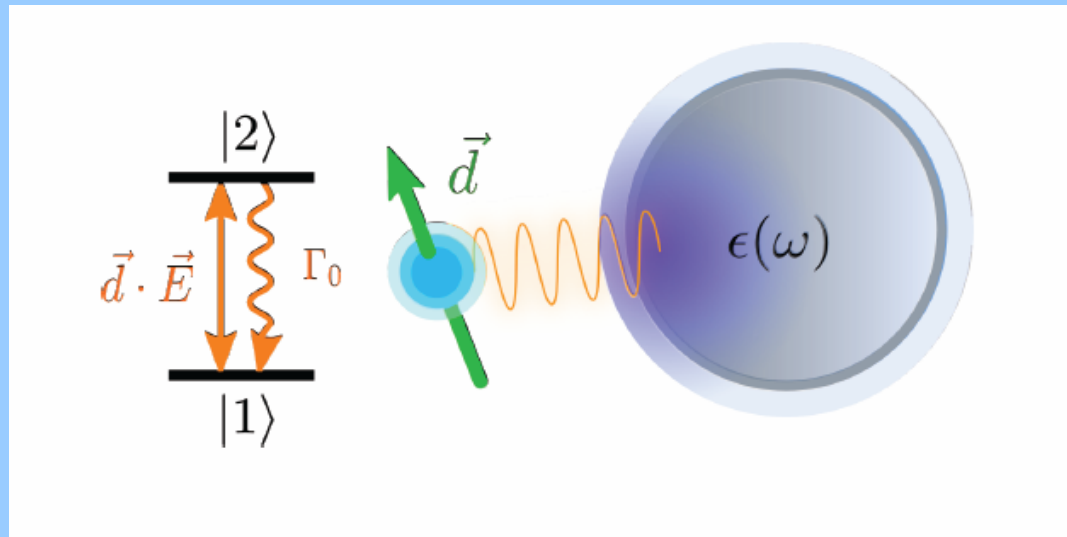
$$F_p = \frac{\Gamma_n}{n_1 \Gamma_0} = \frac{3}{4\pi^2} \left(\frac{\lambda}{n_1} \right)^3 \operatorname{Re} \left(\frac{Q_n}{V_n} \right)$$



$$\begin{aligned} F_p &\sim 35 \\ Q &\sim 10 \\ \operatorname{Re}(V) &\sim 0.01 \left(\frac{\lambda}{n} \right)^3 \\ \operatorname{Im}(V) &\sim 0.001 \left(\frac{\lambda}{n} \right)^3 \end{aligned}$$

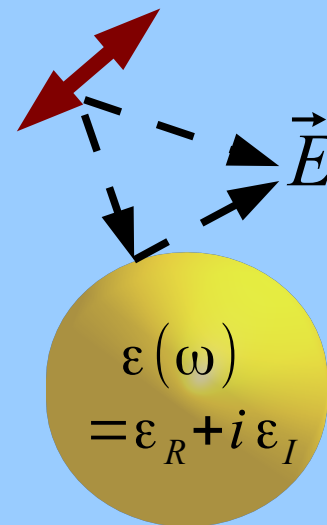
$$\begin{aligned} \frac{\langle \Gamma_n \rangle}{n_1 \Gamma_0} &= \frac{(2n+1)}{3} F_p \frac{(\omega_n / \omega_{em})^2}{1 + 4 Q^2 \delta \tilde{\omega}^2} \left[1 + 2Q\delta \tilde{\omega} \frac{\operatorname{Im}(V_n)}{\operatorname{Re}(V_n)} \right] \\ \delta \tilde{\omega} &= \frac{\omega_{em} - \omega_n}{\omega_{em}} \end{aligned}$$

Quantum plasmonics cQED description



Towards plasmon quantization

Classical description –
dipolar scattering



$$\vec{E}(\vec{r}) = \frac{k_0^2}{\epsilon_0} \bar{G}(\vec{r}, \vec{r}_0, \omega) \cdot \vec{p}$$

Quantization in an
absorbing/dissipative medium –
electric-field operator

$$\hat{E}(\vec{r}) = ik_0^2 \sqrt{\frac{\hbar}{\pi \epsilon_0}} \int d\vec{r}' \sqrt{\epsilon_I} \bar{G}(\vec{r}, \vec{r}', \omega) \hat{f}_\omega(\vec{r}')$$

Gruner, Welsch, PRA 53, 3 (1996)

Plasmon resonances

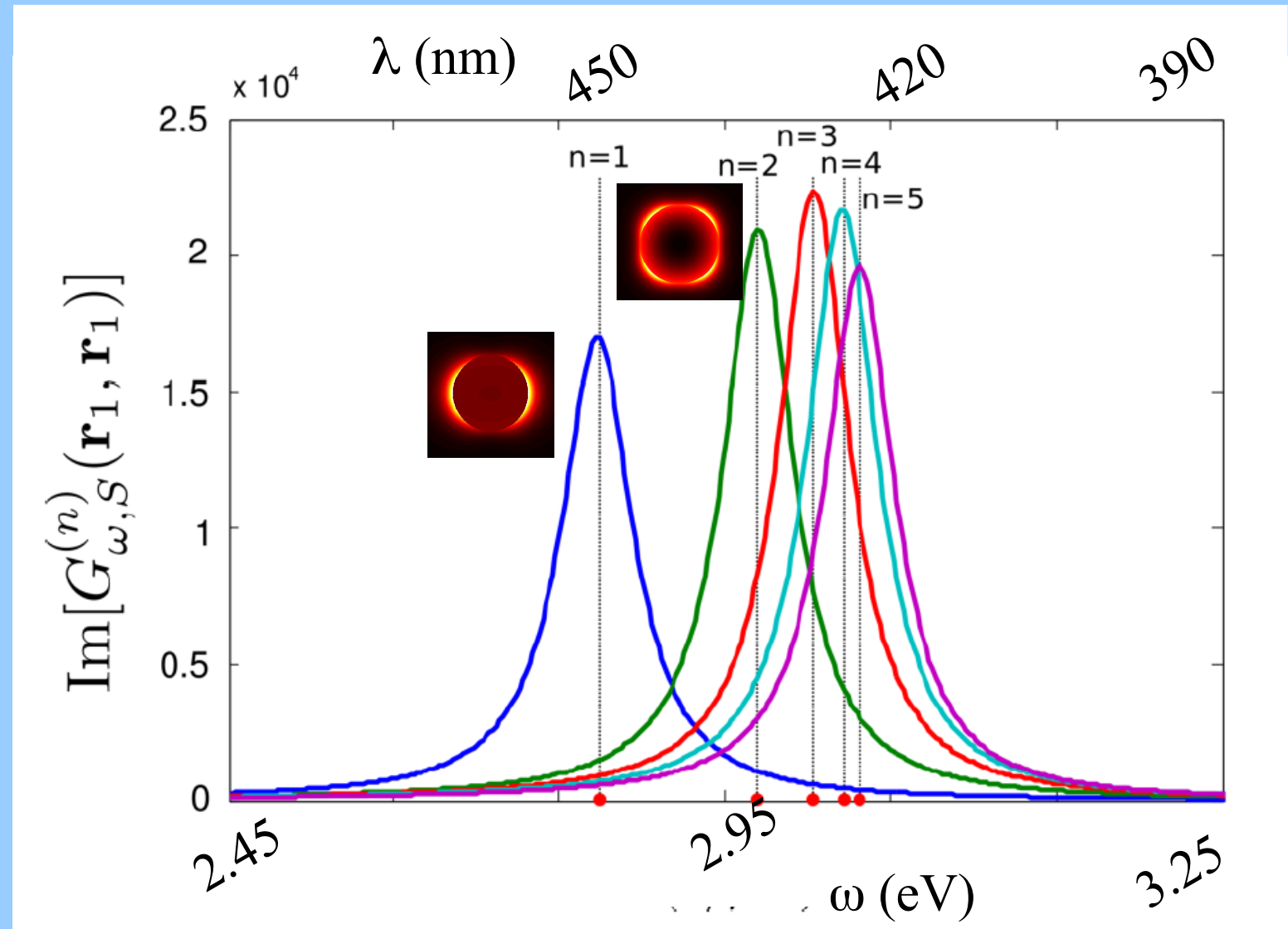
Modal expansion
(Mie formalism)

$$G = G_0 + G_S$$

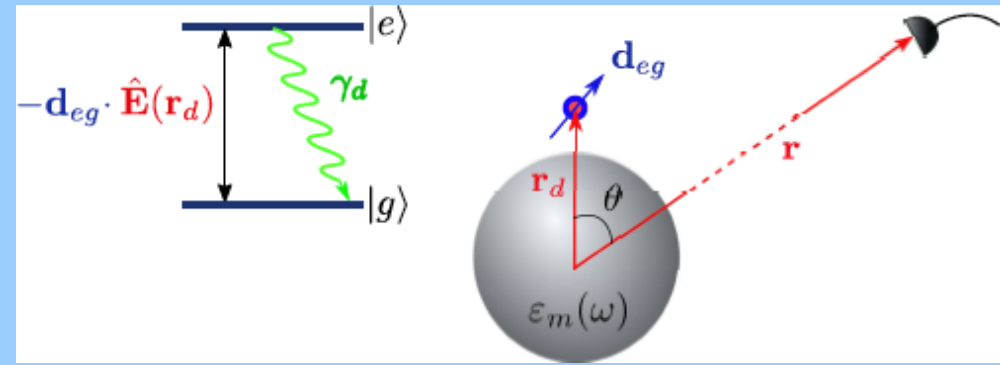
$$G_S = \sum G_S^{(n)}$$

Density of modes

$$LDOS \propto \text{Im } G$$



Quantum plasmonics



$$|\psi(t)\rangle = C_e(t)e^{-i\omega_e t}|e\rangle|\emptyset\rangle + \int d\mathbf{r} \int_0^\infty d\omega e^{-i(\omega+\omega_g)t} \mathbf{C}_g(\mathbf{r}, \omega, t) \cdot |g\rangle|1(\mathbf{r}, \omega)\rangle$$

$$\hat{H}_{QD} = \sum_{i=1}^2 \hbar\omega_{i1}\hat{\sigma}_{ii} - i\hbar\frac{\gamma_0}{2}\hat{\sigma}_{22}$$

Quantum
plasmonics

cQED

$$\hat{H}_R = \int d\mathbf{r} \int_0^{+\infty} d\omega \hbar\omega \hat{\mathbf{f}}^\dagger(\mathbf{r}, \omega) \cdot \hat{\mathbf{f}}(\mathbf{r}, \omega)$$

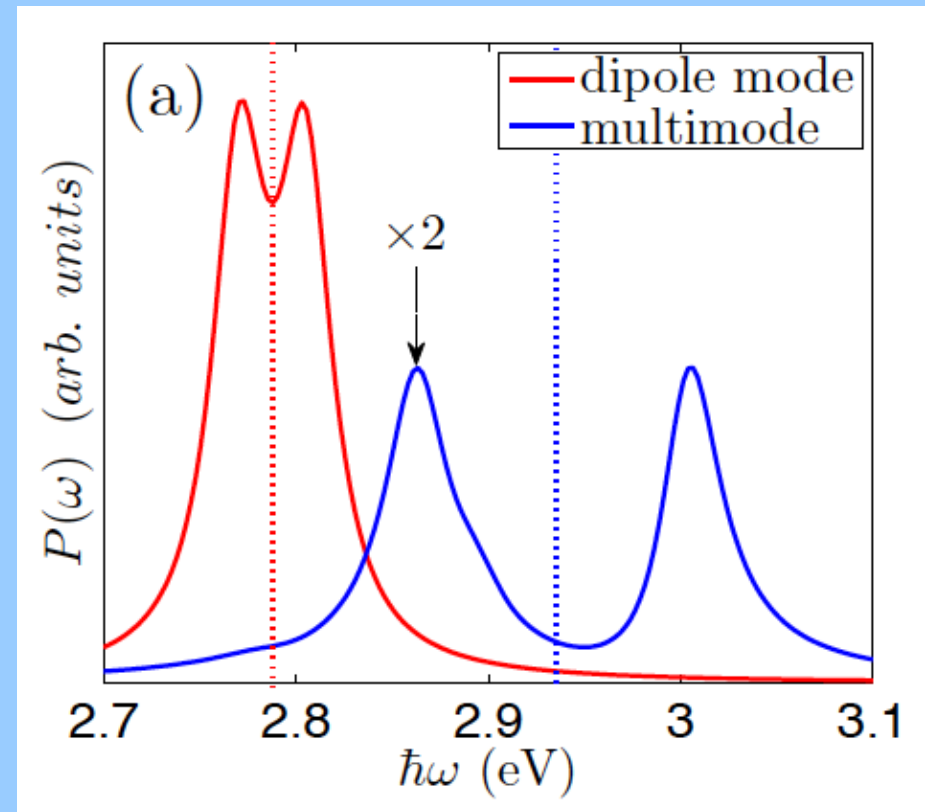
$$\hat{\mathbf{f}}^\dagger(\mathbf{r}, \omega)|\emptyset\rangle = |\mathbf{1}(\mathbf{r}, \omega)\rangle \iff \hat{a}^\dagger|\emptyset\rangle = |1\rangle$$

$$\hat{H}_I = \left[\hat{\sigma}_{21} \int_0^{+\infty} d\omega \mathbf{d}_{21} \left(\hat{\mathbf{E}}(\mathbf{r}_d, \omega) + H.c. \right) \right] \rightarrow \hat{\mathbf{E}}(\mathbf{r}, \omega) = i\sqrt{\frac{\hbar}{\pi\epsilon_0}} \frac{\omega^2}{c^2} \int d\mathbf{r}' \sqrt{\epsilon_I(\mathbf{r}', \omega)} \underline{\mathbf{G}(\mathbf{r}, \mathbf{r}', \omega)} \underline{\hat{\mathbf{f}}(\mathbf{r}', \omega)}$$

Strong coupling

Polarization (near field) spectrum

$$P(\omega) = \langle \hat{\sigma}_{ge}^\dagger(\omega) \hat{\sigma}_{ge}(\omega) \rangle$$
$$P(\omega) = \left| \frac{1}{\omega_{eg} - \omega - i \frac{\gamma_d}{2} - \frac{k_0^2}{\hbar \epsilon_0} d_{eg}^2 G_{uu}^{scatt}(\mathbf{r}_d, \mathbf{r}_d, \omega)} \right|^2$$



Effective model – modal analysis

$$\hat{H}_I = \left[\hat{\sigma}_{21} \int_0^{+\infty} d\omega \mathbf{d}_{21} \cdot \hat{\mathbf{E}}(\mathbf{r}_d, \omega) + H.c. \right]$$



$$\hat{H}_I = i\hbar \int_0^{+\infty} d\omega \sum_{n=1}^N (\kappa_n^*(\omega) \hat{b}_{\omega,n}^\dagger \hat{\sigma}_{12} - \kappa_n(\omega) \hat{b}_{\omega,n} \hat{\sigma}_{21})$$

$$\hat{\mathbf{E}}(\mathbf{r}, \omega) = i \sqrt{\frac{\hbar}{\pi \epsilon_0}} \frac{\omega^2}{c^2} \int d\mathbf{r}' \sqrt{\epsilon_I(\mathbf{r}', \omega)} \mathbf{G}(\mathbf{r}, \mathbf{r}', \omega) \hat{\mathbf{f}}(\mathbf{r}', \omega)$$

Structure of the coupling for each plasmon mode

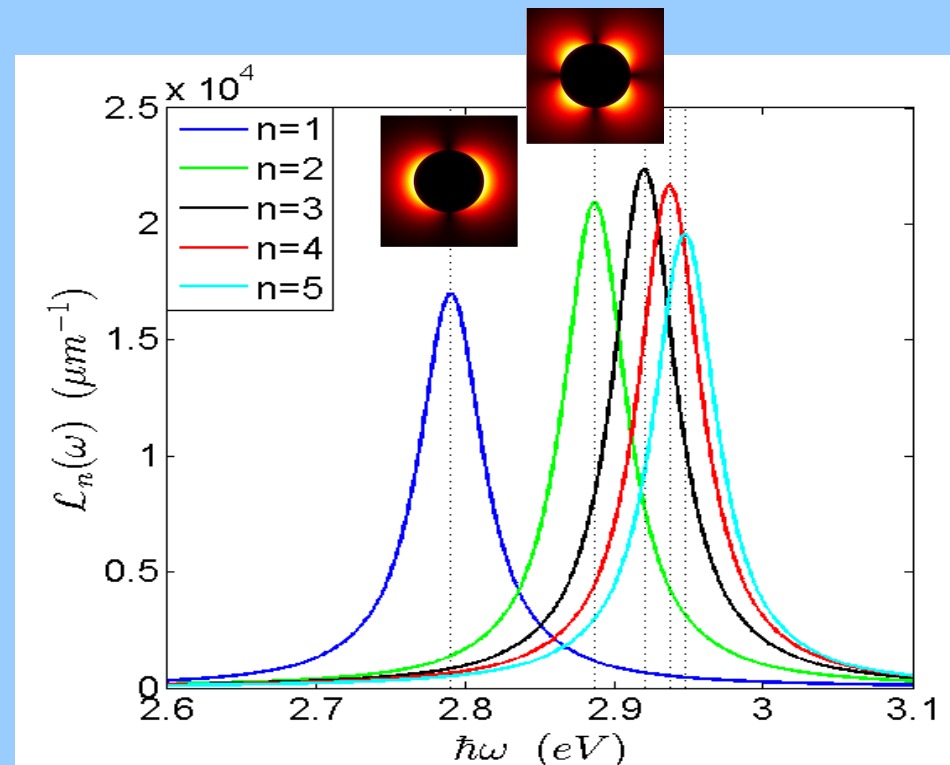
Structure of the coupling

Connection between effective model and Green's tensor :

$$\sum_{n=1}^N |\kappa_n(\omega)|^2 = \frac{1}{\hbar\pi\epsilon_0} \frac{\omega^2}{c^2} \mathbf{d}_{21} \cdot (Im[\mathbf{G}(\mathbf{r}_d, \mathbf{r}_d, \omega)] \mathbf{d}_{21}^*)$$

Lorentzian fitting of the plasmon modes

$$\kappa_n(\omega) = \sqrt{\frac{\gamma_n}{2\pi}} \frac{g_n}{\omega - \omega_n + i\frac{\gamma_n}{2}}$$



Quantum plasmonics – Effective hamiltonian

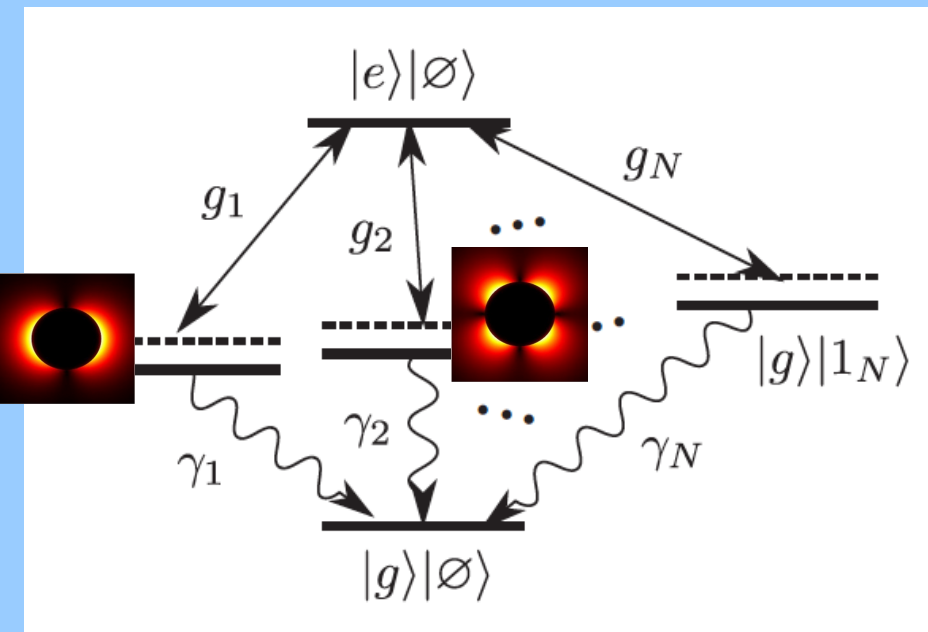
$$\hat{H}_I = i\hbar \int_0^{+\infty} d\omega \sum_{n=1}^N (\kappa_n^*(\omega) \hat{b}_{\omega,n}^\dagger \hat{\sigma}_{12} - \kappa_n(\omega) \hat{b}_{\omega,n} \hat{\sigma}_{21})$$

$$\kappa_n(\omega) = \sqrt{\frac{\gamma_n}{2\pi}} \frac{g_n}{\omega - \omega_n + i\frac{\gamma_n}{2}}$$

↓
Integral

$$H_{eff} = \hbar \begin{bmatrix} -i\frac{\gamma_0}{2} & ig_1 & ig_2 & \cdots & ig_N \\ -ig_1 & \Delta_1 - i\frac{\gamma_1}{2} & 0 & \cdots & 0 \\ -ig_2 & 0 & \Delta_2 - i\frac{\gamma_2}{2} & \ddots & \vdots \\ \vdots & \vdots & \ddots & \ddots & 0 \\ -ig_N & 0 & \cdots & 0 & \Delta_N - i\frac{\gamma_N}{2} \end{bmatrix}$$

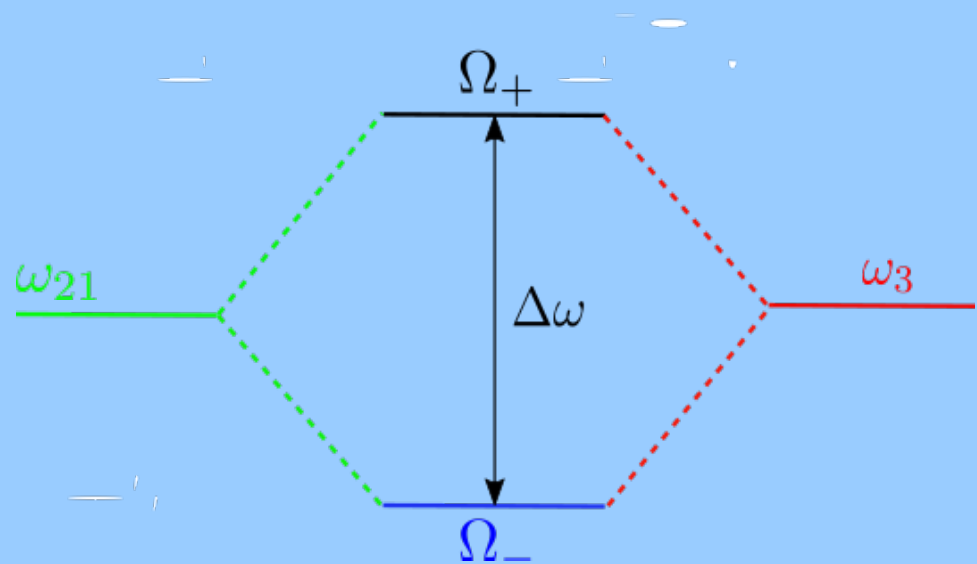
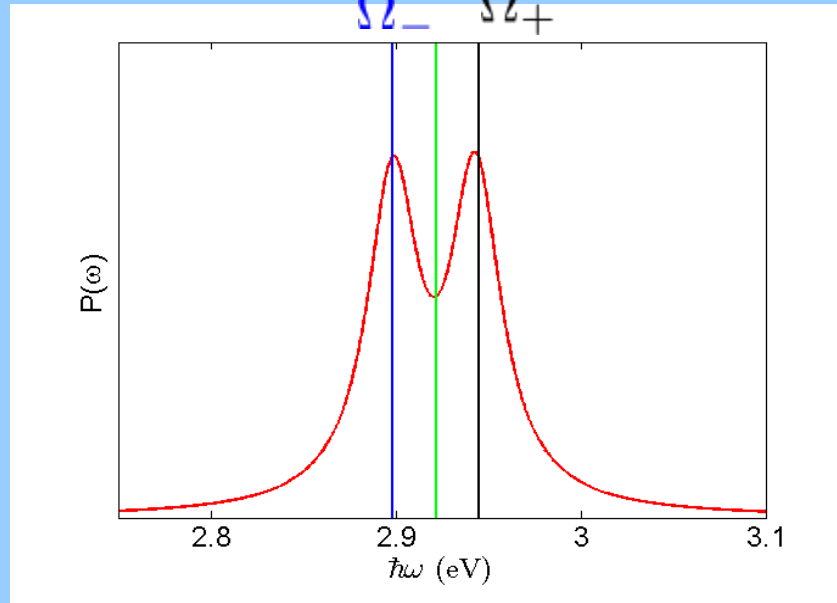
Dressed states



Strong coupling regime

Monomode cavity (LSP₃)

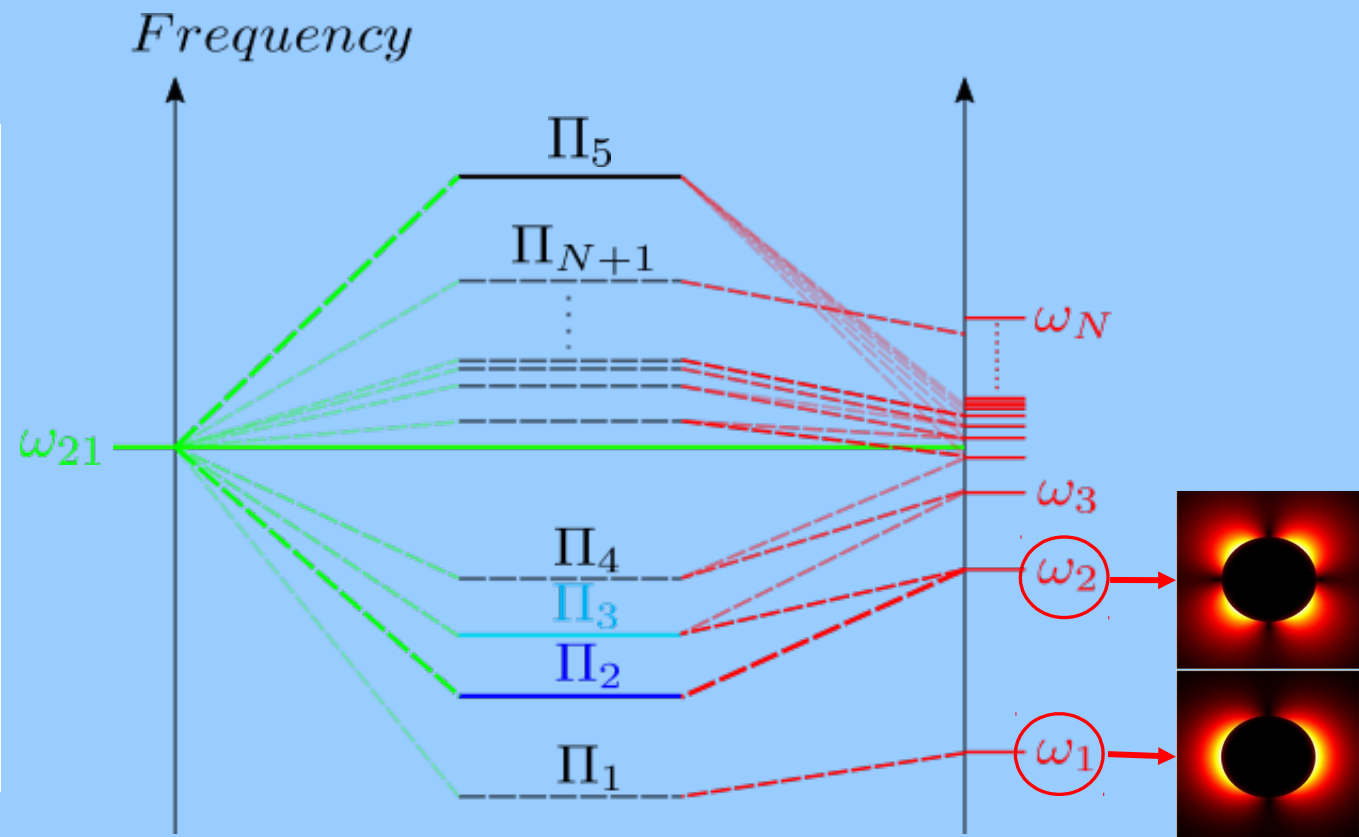
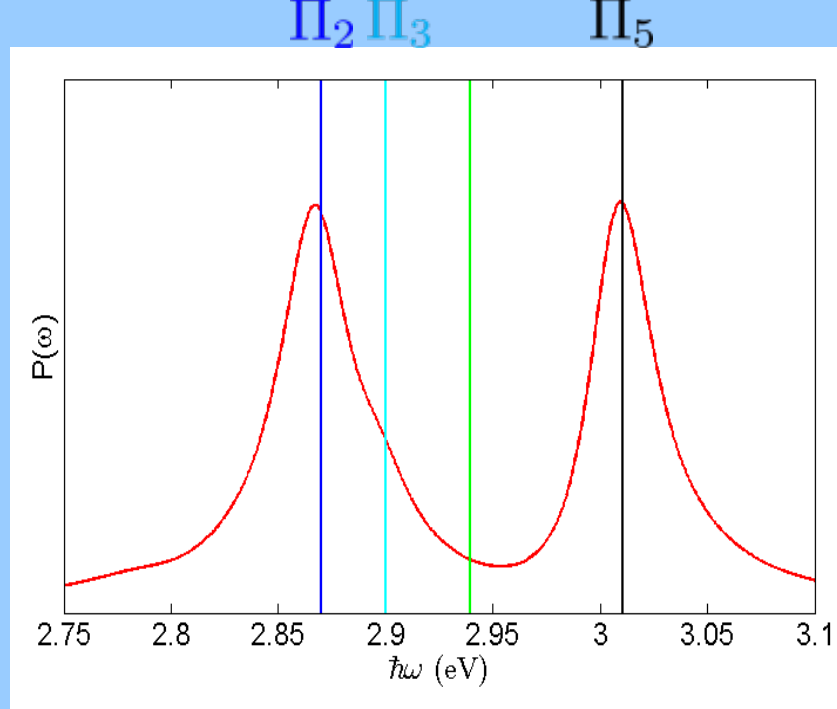
$$H_{eff} = \hbar \begin{bmatrix} -i\frac{\gamma_0}{2} & ig_3 \\ -ig_3 & \Delta_3 - i\frac{\gamma_3}{2} \end{bmatrix}$$



$$\Omega_{\pm} = \omega_{21} \pm \sqrt{g_3^2 - \left(\frac{\gamma_3 - \gamma_0}{4}\right)^2}$$

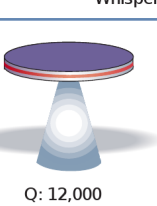
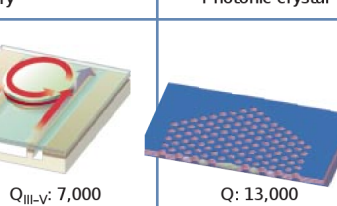
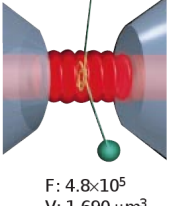
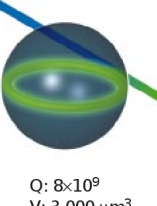
Strong coupling regime

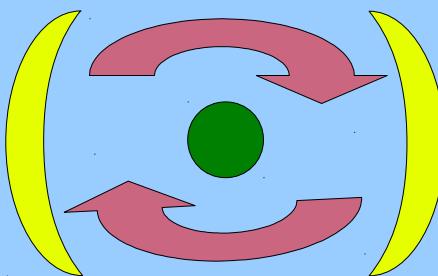
Multimodal lossy cavity (LSPs)



Conclusion

Cavity quantum electrodynamics (cQED)

	Fabry-Perot	Whispering gallery	Photonic crystal
High Q	 <p>Q: 2,000 V: $5 (\lambda/n)^3$</p>	 <p>Q: 12,000 V: $6 (\lambda/n)^3$</p>	 <p>Q_{III-V}: 7,000 Q_{Poly}: 1.3×10^5</p>
Ultrahigh Q	 <p>F: 4.8×10^5 V: $1,690 \mu\text{m}^3$</p>	 <p>Q: 8×10^9 V: $3,000 \mu\text{m}^3$</p>	 <p>Q: 10^8</p>

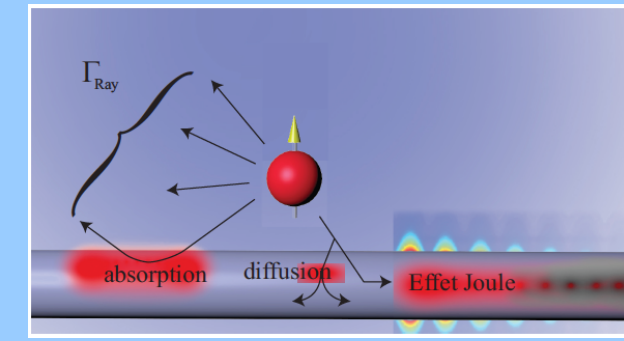


*Duration of interaction
(high Q)*

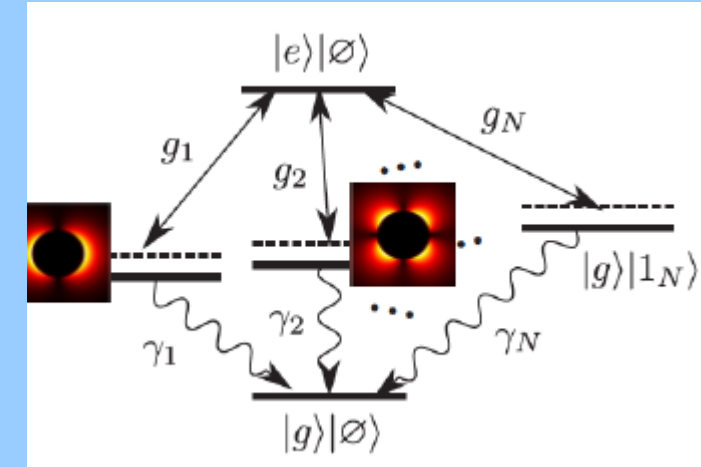
Purcell factor

$$F_p = \frac{\Gamma}{n_1 \Gamma_{tot}} = \frac{3}{4\pi^2} \left(\frac{\lambda}{n_1} \right)^3 \frac{Q}{V_{eff}}$$

Quantum plasmonics (cavityless QED)



*Volume of interaction
(sub-λ)*



Thanks to

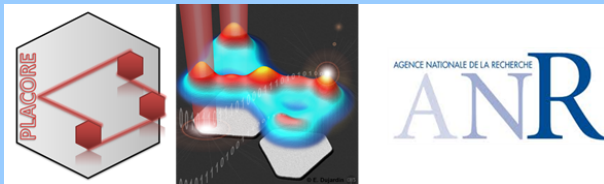
ICB *Nanophotonics & plasmonics*

J. Barthes
S. Derom
A. Bouhelier
J.-C Weeber
A. Dereux

B. Rousseaux
H. Varguet
D. Dszotjan

ICB *Quantum control*

H. Jauslin
S. Guérin



ANR
QDOTICS

